Low-frequency Stimulation Inducible Long-term Potentiation at the Accessory Olfactory Bulb to Medial Amygdala Synapse of the American Bullfrog

by

Geoff deRosenroll
B.Sc., University of Victoria, 2011

A Thesis Submitted in Partial Fulfillment
of the Requirements for the Degree of

MASTER OF SCIENCE

in the Department of Biology

Supervisory Committee

Low-frequency Stimulation Inducible Long-term Potentiation at the Accessory Olfactory Bulb to Medial Amygdala Synapse of the American Bullfrog

by

Geoff deRosenroll
B.Sc., University of Victoria, 2011

Supervisory Committee

Dr. Kerry R. Delaney (Department of Biology)
Supervisor

Dr. Gautam B. Awatramani (Department of Biology)
Departmental Member

Dr. Brian R. Christie (Department of Biology)
Departmental Member

Abstract

Supervisory Committee
Dr. Kerry R. Delaney (Department of Biology)
Supervisor
Dr. Gautam B. Awatramani (Department of Biology)
Departmental Member
Dr. Brian R. Christie (Department of Biology)
Departmental Member

The mitral cells of the accessory olfactory bulb (AOB) of anuran frogs project their axons directly to the medial amygdala (MeA) along the accessory olfactory tract. An *en bloc* preparation of the telencephalon of the American bullfrog *Lithobates catesbeiana* was utilized to study a form of low-frequency inducible long-term potentiation (LTP) expressed at the synapse formed between the terminals of the accessory olfactory tract and the neurons of the MeA. Delivery of repetitive 1Hz-stimulation or sets of 5Hz tetani to the accessory olfactory tract both induced potentiation that was stable for over an hour, as measured by extracellular field recordings. LTP induced by 5Hz tetanus was associated with a decrease in paired-pulse ratio, which would be consistent with an increased probability of release contributing to the increased synaptic strength. Blockade of neither NMDA nor kainate glutamate receptors, with AP5 and UBP310 respectively, prevented LTP induction by 5Hz tetanus; however expression of LTP was partially masked in the presence of UBP310. These results suggest that kainate receptors are involved in the expression of LTP at the AOB-MeA synapse, though the means by which LTP is induced remains unclear.

Table of Contents

List of Figures

List of Abbreviations

ACSF	Artificial cerebral spinal fluid
AOB	Accessory olfactory bulb
AOT	Accessory olfactory tract
AMPAR	α-amino-3-hydroxy-5-methyl-4-isoxazolepropionic acid receptor
$[Ca^{++}]_i$	Intracellular free calcium concentration
cAMP	Cyclic adenosine monophosphate
CV	Coefficient of variation
EPSC	Excitatory post-synaptic current
mEPSC	Miniature excitatory post-synaptic current
fEPSP	Excitatory post-synaptic field potential
ISI	Inter-stimulus interval
KAR	Kainate glutamate receptor
LTP	Long-term potentiation
MeA	Medial amygdala
mGluR	Metabotropic glutamate receptor
MOB	Main olfactory bulb
NMDAR	*N*-methyl-D-aspartate glutamate receptor
PPR	Paired-pulse ratio
PTP	Post-tetanic potentiation
SEM	Standard error of the mean

Acknowledgments

Thank you Dr. Kerry R. Delaney for inspiring me to study synaptic physiology and imparting some small measure of your wisdom on the subject and practical know-how to me. I would also like to thank my committee members Dr. Gautam Awatramani and Dr. Brian Christie, as well as my lab neighbour Dr. Raad Nashmi for providing additional insight and support that has helped to round out my Neuroscience education.

Thank you to my peers in the Neuroscience program and the Delaney lab who have provided me with friendship and inspiration over the years.

Dedication

To my teachers, peers, family, friends, sangha and of course Toby.

Chapter 1 – Introduction

1.1 Olfaction

In most non-primate terrestrial vertebrates two parallel systems handle the sense of smell: the main olfactory and accessory olfactory systems. The main olfactory system, which begins with a large air filled cavity housing the olfactory epithelium, detects airborne odourants that make up the majority of an animal's smell-scape. Operating in parallel, the accessory olfactory system starts with the vomeronasal organ (VNO) — or Jacobson's organ — which is a smaller fluid filled cavity that detects large molecules such as proteins that have been dissolved in mucous and pumped to the epithelium. Non-volatile pheromones excreted by members of the same species or by predators are the most important signals the vomeronasal organ is responsible for detecting given their direct ties to evolutionary fitness, survival and reproduction. Many of the chemical cues picked up from these two sources are able to evoke innate non-learned responses that are present from birth and independent of experience. A recent experiment that compromised the integrity of mouse vomeronasal organs underscored the extent to which the accessory olfactory system is relied on for predator avoidance (Papes et al., 2010). When key receptors of the accessory olfactory epithelium were chemically ablated, mice investigated an anaesthetized rat, a natural predator which naïve mice innately know to avoid, without fear or cautious behaviour. In the absence of accessory olfactory sensation, main olfactory and visual cues failed to elicit aversion on their own (Papes et al., 2010). Thus, the accessory olfactory system is important for the survival and fitness of those species that rely on it for unambiguous detection of threats without prior exposure.

Given the non-volatile media in which the heavy molecules and proteins sensed by the VNO reside, the accessory olfactory system must be attuned to detection of low concentrations and subtle spatial gradients. There is evidence that the main (MOB) and

accessory (AOB) olfactory bulbs differ in how they respond to repetitive activation of the axons coming from the nose. It has been shown in an *en bloc* preparation of the frog brain that short-term plasticity in each of the bulbs is opposite in polarity (Delaney et al., 2009). Whereas the MOB responds to repetitive stimulation of olfactory afferents with depression, the AOB responds to the same stimulation of vomeronasal afferents with facilitation. This suggests that the accessory olfactory system sensitizes to persistent odourants, rather than tuning them out as the main olfactory system does.

The olfactory system is unique among sensory systems in that it has direct connections from the primary sensory processing areas (the main and accessory bulbs) to associative areas of the brain and it bypasses the thalamus, which relays information for other sensory modalities to higher processing in the cortex. In the case of the accessory olfactory system, the mitral cells of the AOB project axons directly to the amygdala, a region implicated strongly in fear learning, fear expression, and motivation (Adolphs et al., 1995). If the AOB network is specialized to respond to persistent stimuli, perhaps its projections to the amygdala also display facilitatory plasticity. This thesis explores activity-dependent plasticity at the synapse between the AOB and the medial amygdala (MeA), the sole terminus of the accessory olfactory tract (AOT) in anuran frogs.

1.2 Plasticity

The central nervous system uses a vast array of tools to modify how it responds to incoming information. The capacity for the system to change, popularly referred to as plasticity, describes the short- and long-term changes in neurons that allow them to act in new ways given the same stimuli. Chemical synapses formed between neurons are where a bulk of the information transfer occurs in the brain, and these synapses provide the most direct site for modifications to the signal being carried. Every one of these connections have pre- and post-synaptic sides, both of which are subject to changes that can strengthen or weaken the transfer of information. Thus any changes in the response of a post-synaptic neuron to a given stimuli must be investigated while considering both sides of the synapse. Much of the research to date has been focused on events occurring post-

synaptically and the first experiments on long lasting synaptic plasticity discovered a phenomenon dependent on post-synaptic mechanism.

The first account of long-term potentiation (LTP), generally defined as synaptic enhancement lasting longer than an hour, was discovered in the hippocampus by Bliss and Lømo in 1973. Delivery of 20 Hz tetanic stimulation to the perforant path of anaesthetized rabbits induced a persistent increase in the response of dentate granule cells to further stimulations of their perforant path afferents. It was found years later that *N*-methyl-D-aspartate glutamate receptor (NMDAR) played a prominent role in the induction of this potentiation (Malenka, 1991; Bliss and Collingridge, 1993). The NMDAR presents a particularly attractive model mechanism for Hebbian learning, which until hippocampal NMDAR-dependent LTP was discovered, had no physiological examples or correlates to back up the concept (Kelso et al., 1986).

The NMDAR only opens to allow non-specific cation flux — Na^{+}, K^{+}, and most importantly Ca^{++} — when multiple conditions are met: glutamate binding, glycine binding, and membrane depolarization. At resting membrane potentials, the NMDAR channel pore is physically blocked by a Mg^{++} ion from the extracellular side. When the electromagnetic force exerted on the Mg^{++} ion by the negatively charged inner membrane decreases sufficiently it is free to diffuse out of the channel. Thus, even if the ligand binding domains of the receptor are occupied, cation flux will not occur unless the membrane is sufficiently depolarized, with appreciable unblocking occurring at -20mV and increased permeability at more positive voltages (Nowak et al., 1984). Therefore the pre-synaptic cell must release the neurotransmitter glutamate into the cleft while the post-synaptic cell is receiving sufficient input from the same, or some combination of sources, to be depolarized enough to relieve the divalent cation block. This closely mirrors the Hebbian model of a neuron becoming more effective at driving another neuron to fire if it repeatedly takes part in the firing of that neuron (Kelso et al., 1986).

In the case of the traditional LTP induction method, where high-frequency tetanus (> 10Hz) is delivered to the pre-synaptic neuron, the condition of coincident pre- and

post-synaptic activation is met from a single source. Action potentials follow each other so closely in this scenario that glutamate enters the cleft while the post-synaptic neuron continues to be depolarized by the α-Amino-3-hydroxy-5-methyl-4-isoxazolepropionic acid receptor (AMPAR) channels that had been opened by the preceding of glutamate release events. This method works quite well for induction of NMDAR-dependent LTP in the hippocampus, but it is not unique. Since the landmark studies on LTP, other methods designed to more closely mimic physiological processes and associativity, have been developed and used in the hippocampus and other brain areas. These various non-tetanic stimulation protocols have successfully induced both NMDAR-dependent and -independent forms of LTP (Habib and Dringenberg, 2010a; Feldman, 2012; Larson and Munkácsy, 2014).

Induction of LTP by much slower stimulation frequencies (*e.g.* < 10Hz) has received more attention in the last 15 years, particularly in the CA1 region of the hippocampus and the amygdala (Li et al., 2001; Lanté et al., 2006; Huang and Kandel, 2007). Repeated stimulation at frequencies as low as 1Hz are able to induce LTP through various glutamate receptor (NMDAR, KAR, group 1 mGluR) and neuromodulator-dependent (5-HT, DA, beta-adrenergic) mechanisms in several areas of the brain. Despite the differences in stimulus paradigms required to induce these potentiation events, many of the downstream cellular secondary mechanisms and messengers responsible for expressing the changes in synaptic function are shared. For example, rises in intracellular free calcium concentration ($[Ca^{++}]_i$) and the activation of protein kinase A (PKA) are commonly important for many of these alternate forms of LTP, pointing to significant overlap between the underlying biochemical infrastructures that neurons use for activity-dependent plasticity (Li et al., 2001; Lanté et al., 2006; Huang and Kandel, 2007; Shin et al., 2010). The proteins themselves are agnostic to whatever events meet their conditions of activation, so any number of manipulations, natural or otherwise, might lead to LTP.

That long-term potentiation does not solely exist as a putative mechanism for associative-learning bears remembering and should be clear from how easily it can be induced without any temporally conjunctive events taking place. If one pre-synaptic

input, in the absence of others, can lead to an increase in the post-synaptic response to itself, this could be described as more of a non-associative sensitization effect than a learning/association one. The temporal lobe and particularly the amygdaloid bodies that it houses, provide a strong example of pathological sensitization and excitability. These regions are home to the "kindling" phenomenon, wherein repetitive stimulation results in hyper-excitability of a network, that can lead to the expression of epileptic seizures (Goddard et al., 1969). Therefore, the possibility exists that persistent non-associative changes in synaptic strength are part of normal non-pathological functions of this brain region.

1.3 The amygdala

Amygdala is the name given to a set of nuclei located medially in the temporal lobe and historically considered to be a part of the limbic system (Laberge et al., 2006). The amygdala has long been associated with emotion, motivation and aspects of memory especially pertaining to matters of survival. Humans with amygdala lesions suffer from a wide range of impairments, including the inability to recognize the expression of fear in others' faces (Adolphs et al., 1995). Like the hippocampus, the amygdala has proven to be a plastic region that expresses LTP and given that it hosts a convergence of information from multiple sensory modalities, it is a suitable place to study the physiological basis of Hebbian learning in the context of fear (Pape and Pare, 2010). A key function of the amygdala is forming associations between neutral stimuli and aversive stimuli, such that the neutral stimuli itself can evoke fear of harmful events that it comes to predict, and the amygdala's ablation can limit an animal's ability to perform fear learning (LeDoux et al., 1988).

While learning associations between stimuli in the environment that may aid in the survival of the organism is a very important function, the same synaptic machinery that underlies associative conditioning can also participate in potentiation events that seem to have no associative requirement. In rodent brain slices, frequencies of

stimulation as low as 1Hz delivered to axons of the external capsule projecting into the basolateral amygdala have been shown to potentiate not only the synapses that their own terminals make, but also terminals of projections coming from the basal amygdala (Li et al., 2001). While this activity-dependent physiological change could very well participate in behavioural learning, it might not play a role in learning at all. The glutamate receptor channels responsible for the heterosynaptic facilitation reported by Li et al. were kainate receptors (KAR), which have a large presence in the amygdala and are the primary culprits in the kindling phenomenon (Fritsch et al., 2014).

These issues are important to keep in mind, as the present study is concerned with a form of LTP in the medial amygdala (MeA) of the American bullfrog, *Lithobates catesbeiana*, evoked by repetitive low-frequency (1-5Hz) stimulation to the accessory olfactory tract (AOT) in a non-associative, single input, manner. A benefit of working with a frog model is that the telencephalon remains largely intact, including the whole amygdala, so long range projections and the entirety of target cells are intact. However, for the same reason, issues such as network sensitization and kindling could always be confounding factors for experiments hoping to examine synaptic physiology. Thus, while the potentiation we observe in the MeA could be theorized to reflect a sensitization to a persistent odour in the environment, there is reason to be apprehensive about assigning meaning the physiology.

1.4 Benefits of using a frog animal model for mammalian brain function

Modern neuroscience relies heavily on the nervous tissue of the mouse and rat to provide insights into the mammalian nervous system. While more and more advanced techniques are allowing functional studies to be carried out *in vivo*, much of the work remains *in vitro* with the use of brain slices, most typically along the coronal or sagittal planes. Slicing the brain simultaneously allows researchers access to their cells of interest both optically and physically and makes the tissue easier to maintain with controlled temperature and solute/oxygen concentrations throughout experiments. However, the

process of cutting sections of tissue introduces problems that create a rift between the physiology observed in the experimental context and the physiology of living animal's brains. Attempting to generalize and draw causal relationships between what we observe in the dish and what occurs *in situ* can be more difficult when there are confounds that result from the preparation of the nervous tissue before data collection begins.

Slicing through nervous tissue can cause damage to not only the neurons of interest, severing their long range projections or their dendritic arbours that may extend perpendicular to the plane of slicing, but also to the neighbouring neurons and the overall network. When neurons are damaged or transiently deprived of oxygen or glucose there can be large amounts of glutamate released by the dying or unhealthy cells before glia move in to control damage and begin the repair process (Steven, 1984; Faden et al., 1989; Katayama et al., 1990). The damage driven increase in activity can cause excitotoxicity, leading to further cell death resulting from excessive Ca^{++} and anion influx (Choi, 1987).

Complications with maintaining the health of cells in slices mean that experimenters have limited time set by a number of factors including slice thickness, sensitivity of the tissue, drug application and the invasiveness of the chosen recording method. Depending on the needs of the study, especially in cases where pre-drug, drug application, and drug removal conditions are paired with electrophysiology, the time window provided by slices can be restrictive and require many animals to collect each successful replication should health deteriorate before completion of experiments. On top of all of these limitations, while the slice provides a way to investigate the behaviour and interactions of single neurons or local networks, the cells are generally cut off from their larger network due to the plane of slicing. Making use of *en bloc*, or more complete tissue preparations from non-mammals can open up new possibilities since they do not suffer from some of the problems that slicing introduces.

Some cuts may be made to *en bloc* preparations in order to allow better access to areas of interest, but the tissue still remains largely intact limiting damage to target cells and regions. Due to the high metabolic demands of mammalian tissue, studies that use

mice or rats as their model do not typically provide the option to use *en bloc* preparations. Other animal models such as amphibians have brains for which slicing can sometimes be forgone. The amphibian brain differs from the mammalian brain in a few key ways that make it better suited to *en bloc* preparations.

As ectotherms, amphibians are able to live with low metabolic rates, contrary to endothermic animals which rely on high metabolisms to maintain their higher stable state body temperatures. Thus their tissue can be kept healthy by working at their normal living temperatures, lower than those used for experiments with mammalian tissue (Delaney and Hall, 1996). Due to their lower average metabolism and cooler working temperatures, amphibian cells require lower quantities of metabolites such as oxygen and glucose, so diffusion rates are not quite as limiting to tissue thickness when relying on superfusion through a dish to maintain them (Berner, 1999). Unburdened by a neocortex, the amphibian forebrain tissue is thinner than that of mammals making brain regions such as the limbic system accessible to the bath without extensive tissue manipulation. One research group using a post-telencephalon preparation of an anuran frog CNS demonstrated brainstem neurons could maintain resting membrane potentials below -40mV after four days of being kept in cool circulated ringer (Luksch et al., 1996). Prolonged survivability is a useful attribute, but the most interesting benefit afforded by *en bloc* preparations is the preservation of long range axonal projections regardless of plane.

Because the brain is not sliced, axons that bridge connections between brain regions (and sensory organs) can be preserved, allowing different stimulation paradigms and observation of more complete network behaviour given that entire regions (e.g. accessory olfactory bulbs and amygdala) can be left intact. Previous work conducted on the leopard frog, *Lithobates pipiens,* CNS has taken advantage of these benefits to investigate responses to artificial and natural primary sensory information in the olfactory bulbs as well as Ca^{++} influx into the terminals of accessory olfactory mitral axons several millimetres from their cell bodies (Delaney and Hall, 1996; Delaney et al., 2001, 2009; Mulligan et al., 2001). The original *L. pipiens* nose-brain preparation provides an

example of how long-lasting amphibian *en bloc* preparations can be, as the researchers reported it to be usable for at least 12 hours (Delaney and Hall, 1996). Research directed at the mechanisms of long-term plasticity would be able to take advantage of this stability and potentially expand our ability to investigate these phenomena in intact tissue with the added freedom of *in vitro* study.

1.5 The accessory olfactory bulb to medial amygdala synapse

Anuran frogs, including *L. pipiens* and *L. catesbeiana*, have direct connections between their olfactory systems and the nuclei of the amygdala. Mitral cells of the bulbs project their axons primarily in two bundles, the lateral olfactory tract from the main bulb and the accessory olfactory tract (AOT) from the accessory bulb (Scalia, 1972; Scalia et al., 1991; Mulligan et al., 2001; Moreno and González, 2003). The AOT forms a direct projection from the AOB to the amygdala without branching off along the way. It projects along the ventromedial wall of the lateral cortex to its sole terminus onto the medial division of the amygdala (Figure 1). Whereas the axons of the lateral olfactory tract project collaterals to locations besides the lateral amygdala, including the medial amygdala and the lateral pallium (Moreno and González, 2004). Due to the tight grouping of the AOT's axons and its single area of termination, the accessory mitral cell to medial amygdala synapse can be a useful model for the study of synaptic transmission and plasticity.

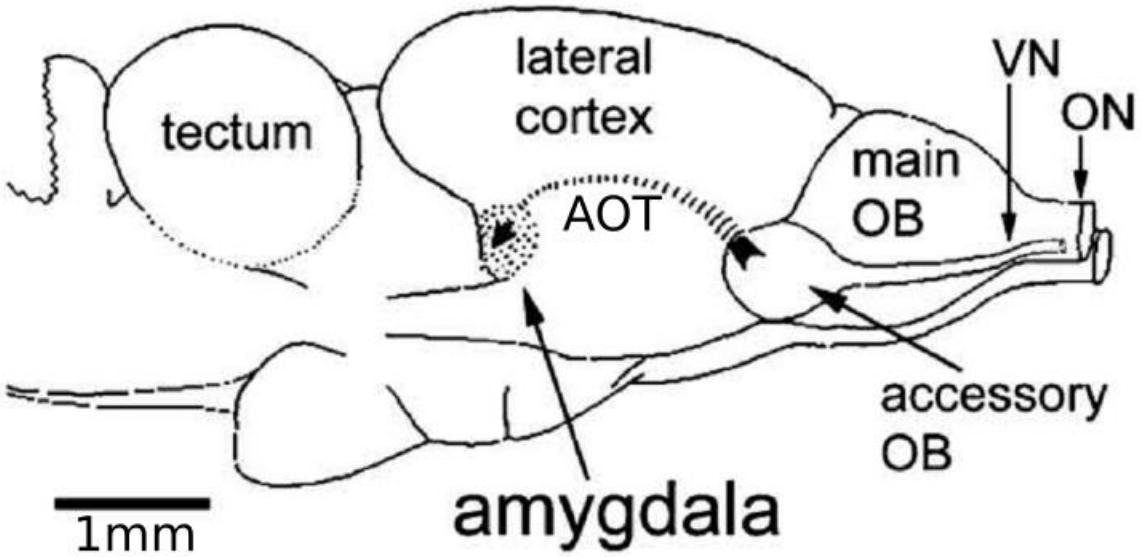

Figure 1. Illustration of the central nervous system of the leopard frog, *Lithobates pipiens*. Adapted from Scalia (1972). AOT, accessory olfactory tract**;** OB, olfactory bulb; ON, olfactory nerve; VN, vomeronasal nerve.

Previous work by Mulligan et al. in 2001 using functional Ca^{++} imaging to observe the Ca^{++}-dependence of vesicle release established the ease of stimulating the tract and recording the post-synaptic field response. Aggregate Ca^{++} influx into the terminals of the tract was easily visualized though the use of dextran-conjugated Ca^{++} indicators, injected into the AOB *in vivo* and allowed to travel down the mitral cell axons overnight (O'Donovan et al., 1993). Due to the tight bundling of AOT axons and the concentrated terminal field in the MeA, the synapse is also suitable for electrophysiological investigations without accompaniment by functional imaging.

The present study made use of a similar *ex vivo* preparation of the American bullfrog, *L. catesbeiana,* telencephalon to investigate a plasticity phenomenon at the AOB-MeA synapse. Repetitive stimulation to the AOT at frequencies of 5Hz and 1Hz were found to elicit potentiation of the MeA field potential that lasted for over an hour. The data were consistent 5Hz induced increase in synaptic strength being partially expressed by an increased probability of neurotransmitter release, suggesting the involvement of both the pre-synaptic and post-synaptic neurons in the expression of this LTP. Antagonists for glutamate receptors that may be involved on either side of the

synapse were used to determine whether the target receptors were required for induction and/or expression of the observed synaptic potentiation. Neither NMDARs nor KARs were individually required for induction of LTP by 5Hz stimulation, however KARs were found to be involved in the expression of LTP. Based on these results, I propose a model in which increased neurotransmitter release and an increased population of KARs in the post-synaptic membrane combine to produce the observed LTP.

Chapter 2 – Methods and Materials

2.1 *In vitro* forebrain preparation

Wild American bullfrogs (*L. catesbeiana)* were caught by hand at Florence Lake (Victoria, British Columbia) and held at the Outdoor Aquatics Unit of the University of Victoria. They were kept under a summer light cycle (16hr on, 8hr off) in tanks supplied by a 15°C flow-through system until being brought to the lab on the day of experimentation.

Frogs were anesthetized with immersion in 2mM tricaine methanesulfonate (MS222) buffered to ~7.4 pH by sodium bicarbonate, until lacking a foot pinch reflex, before rapid decapitation. Following removal of the eyes and skin, skulls were bathed in ice-cold artificial cerebral spinal fluid (ACSF) containing (in mM) 72 NaCl, 26 $NaHCO_3$, 0.5 Na_2HPO_4, 2.5 NaH_2PO_4, 1.5 $MgSO_4$, 2 KCl, 2 $CaCl_2$ and 10 dextrose recently oxygenated via bubbling with carbogen gas (95% O_2 / 5% $C0_2$) that also served to maintain the solution at pH 7.4. Brains were removed, stripped of dura and hemisected in a Sylgard^{TM} lined dish while immersed in iced ACSF. Both hemispheres were then severed caudal to the thalamus and rostral to the optic tectum. Lateral ventricles were cut open along the rostro-caudal axis of the dorsal ridge using fine iris scissors, then a dorsal-ventral cut was made at the caudal end of the lateral ventricle (rostral to the thalamus) to allow access to the inner face of the lateral wall of the ventricle/telencephalon. One hemisphere was transferred to a Sylgard^{TM} lined recording dish, while the other was placed in well-oxygenated circulating ACSF to be used following completion of experiments with the first hemisphere.

Bent minuten pins were used to hold the ventricle open and provide access to the inner face of the lateral wall for electrical stimulation and recording. The AOB and a ridge where the lateral ventricular wall are visible as thicker areas of the tissue (Figure 2A). The AOT projects (indicated by dotted lines in Figure 2A) from the AOB and runs

dorsally over the visible ridge, allowing repeatable accurate electrode placement. The recording dish was then connected to gravity fed (saline drip) carbogen-bubbled ACSF, providing the tissue with continual perfusion at 1-2mL/min.

2.2 Stimulation

Bipolar stimulating electrodes were made with 1.5mm outer diameter borosilicate glass theta tubes. Theta tubes were pulled with a Sutter Instruments Micropipette Puller and broken off to ~250µm diameter. Theta electrodes were completed by filling with ACSF and placement of 125µm teflon-coated silver wire (with ends bared of coating) down each partition. Electrodes were placed on the AOT approximately 100µm posterior to the AOB, as illustrated in Figure 2A. Stimulation currents of 10-500µA at 500µs duration were delivered to the AOT with HEKA Chart Master through an A/D board (Instrutech ITC-18 Data Acquisition Interface) and stimulus isolation unit (Neuro Data SIU90).

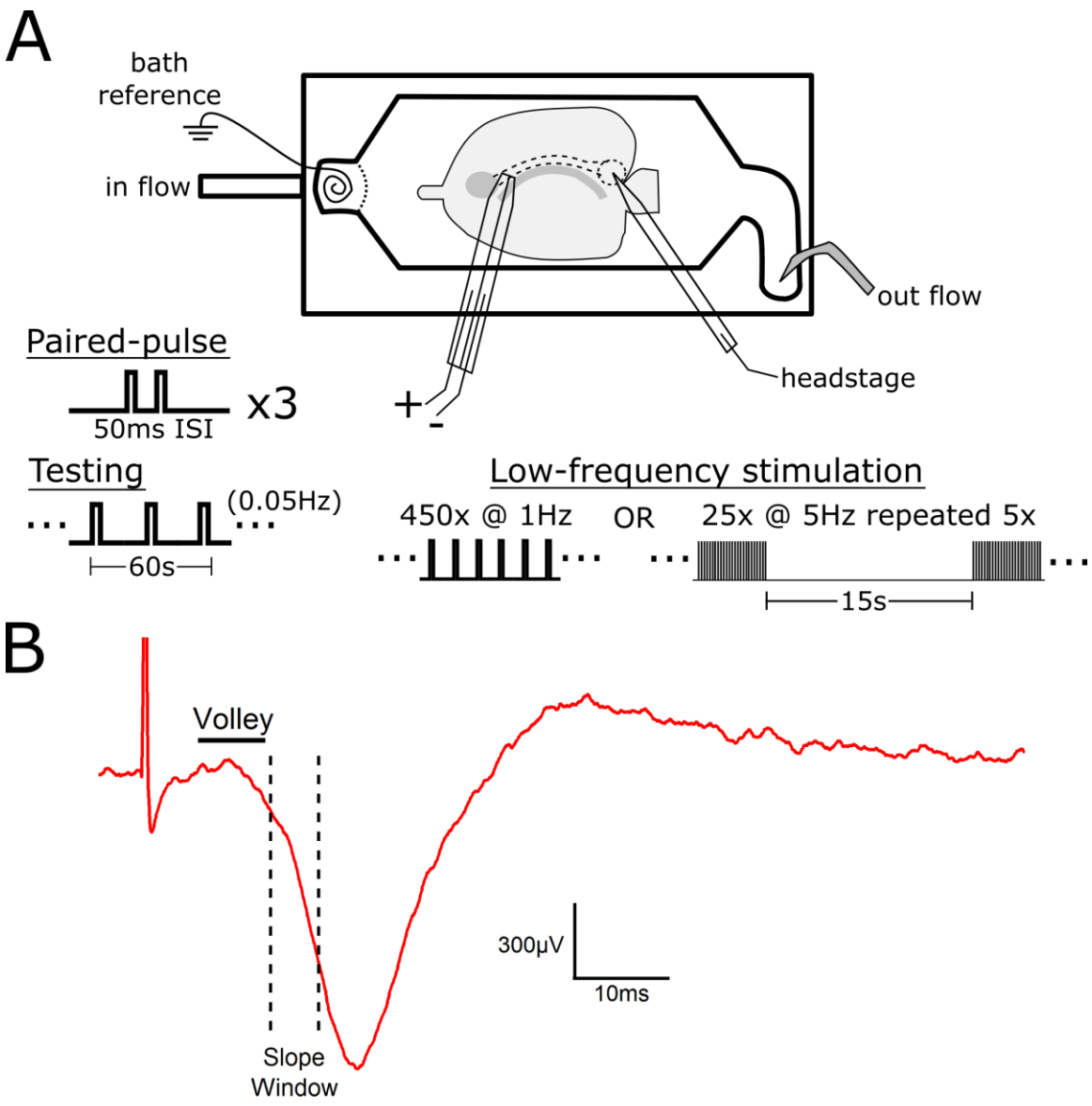

Figure 2. Illustration of experimental setup and synaptic strength quantification. (A) The inner walls of the ventricle are exposed to allow bipolar stimulation of the AOT and extracellular recording of the MeA as shown (AOT and MeA indicated by dotted lines). Bipolar electrodes are used to deliver 500μs square pulse test stimuli to the AOT in the form of 50ms ISI paired-pulses repeated 5x at 1 minute intervals and synaptic strength testing at 0.05Hz for varying lengths of time. Low-frequency stimuli are delivered by the same electrode as either a 7.5 minute train of pulses at 1Hz, or 25 pulses at 5Hz repeated 5x at 15s intervals. (B) Synaptic strength at the AOB-MeA synapse is quantified by the slope of the fEPSP over a 5ms window beginning after the pre-synaptic volley has ended (3ms into rise-time).

Stimulation intensity was adjusted to evoke 1/3 maximal MeA field response at experiment outset. The standard testing protocol consisted of single pulses delivered with 20s inter stimuli intervals (ISI) (0.05Hz) (Figure 2A). At time-points dependent on the current experimental design, 3 sets of 50ms ISI paired-pulse stimuli were delivered with 1 minute rest time between pairs to test paired-pulse ratio (PPR). Repetitive low-frequency conditioning stimulation was operationally achieved with 450 pulses at 1Hz, or 5 sets of 25 pulses at 5Hz with 15s intervals between sets.

2.3 Electrophysiological recording

Excitatory post-synaptic field potentials (fEPSPs) were recorded with low-resistance (< 100 kΩ) ACSF filled broken tipped (1mm outer diameter, 0.58mm inner diameter) borosilicate glass microelectrodes mounted in silver chloride pellet electrode holders. Chlorided silver wire was coiled and submerged in the recording bath to serve as a reference electrode. Recording electrodes were positioned over the MeA and advanced ~250µm below the ventricular surface, adjusted and re-positioned to maximize the negative amplitude of fEPSPs evoked by stimulation to the AOT. fEPSPs were amplified 1000-fold (10x head stage, 100x main amp) and band-pass filtered between 0.1Hz and 1kHz using a custom built amplifier. Analog signals were passed to an Instrutech ITC-18 Data Acquisition Interface where they were digitized at 20k samples/second for acquisition by a MacBook or Acer Laptop running HEKA ChartMaster. Analysis was performed offline using Igor Pro (Wavemetrics, Eugene, OR, USA) and the NeuroMatic plugin.

2.4 Quantification of field potentials

MeA fEPSP recordings pick up pre-synaptic volleys, characterized by a positive-going followed by a negative-going peak, lasting approximately 7ms total. The strength

of the post-synaptic response was quantified by the negative slope over a 5ms window starting 3ms after the beginning of the negative rise of the fEPSP to avoid contamination by the pre-synaptic volley (the negative-going portion of which overlaps with the first 2-3ms of the fEPSP) (Figure 2B). All measured slopes of 0.05Hz synaptic strength testing in a given experiment were normalized to the average of the last 3 minutes of initial (pre-tetanus/pre-drug) synaptic strength testing, referred to as 'Baseline' in all figures displaying slope over time. Averages of normalized slope over 3 minutes of testing (9 traces at 0.05Hz) were used for all statistical comparisons of synaptic strength following drug and tetanic/repeated stimulation treatments.

The ratio of the post-synaptic response to the second action potential (AP) of a pair relative to the first is defined as the paired-pulse ratio (PPR) and can, at many synapses, provide information about the pre-synaptic neuron's release probability (Delaney et al., 1989; Zucker and Regehr, 2002). At synapses with moderate to high initial release probability, a decrease in PPR corresponds to an increase in release probability, as more vesicles being released by the first AP leaves a smaller pool of vesicles available for release by the second AP. In order to determine whether an increased probability of release could be responsible for changes in synaptic strength following 1Hz (or 5Hz) stimulation, PPR was averaged from 3 repeats (one minute intervals) of paired stimuli at 50ms ISI before the train of 1Hz (or 5Hz) stimulation then 30 and 60 minutes afterward for comparison.

PPRs were calculated using the same slope measuring criteria on responses to 50ms ISI paired stimuli. Slopes of secondary pulse fEPSPs were divided by slopes of primary pulse fEPSPs to obtain each individual ratio. Individual ratios were averaged over the 3 repeats recorded at each time point to obtain the final PPRs presented in the results.

2.5 Statistics

All measurements presented in this thesis were made in a before-after paradigm, in which each tissue preparation for a given experiment received the same stimulation and drug treatments. This was done with the intention of comparing the state of the tissue after the chosen treatments, to the state before. Therefore, average fEPSP slopes (synaptic strength testing) and average PPRs calculated for each experiment were analyzed using repeated measures statistics. Repeated-measures analysis of variance (ANOVA) tests were used to verify the independent variables (low-frequency stimulation and receptor antagonists) had some significant effect on the dependent variables measured and to provide information about variability within-treatments. Sphericity was not assumed, therefore Geisser-Greenhouse's epsilon (ε) was calculated and used to correct all repeated-measures ANOVAs performed. If a significant effect was detected, post-hoc two-tailed paired t-tests ($\alpha = 0.05$) were performed between time-points of interest (before and after individual treatments). Significant α levels were adjusted by a post-hoc Bonferroni correction according to the number of statistical comparisons made on an experiment by experiment basis.

2.6 Drugs and delivery

In all experiments, brains were superfused with carbogen (95% O_2 / 5% CO_2) bubbled ACSF via gravity at 1-2mL/min. Fluid entered through the base of the left end of the recording dish and passed around the bath reference electrode coil (creating turbulence) before flowing over the tissue and removed via suction at the far right end of the chamber (Figure 2A).

Aliquots of concentrated drugs were prepared and stored at -20°C then removed to defrost within an hour of experimentation. Aliquots of AP5 (DL-2-Amino-5-phosphonopentanoic acid sodium salt, Abcam) disodium salt were prepared at a concentration of 50mM in ddH_2O and aliquots of UBP310 ((*S*)-1-(2-Amino-2-carboxyethyl)-3-(2-carboxy-thiophene-3-yl-methyl)-5-methylpyrimidine-2, 4-dione,

Tocris Bioscience) were prepared at 10mM in DMSO. DL-AP5 and UBP310 were diluted to concentrations of 100µM and 10µM respectively in ACSF. A manual valve was used to change between reservoirs containing control ACSF and drug ACSF solutions with care paid to maintaining constant flow rate.

Chapter 3 – Results

3.1 Prolonged 1Hz stimulation potentiates AOB to MeA synapse with no evidence for a change in release probability

A long-lasting form of potentiation inducible by low (< 10Hz) frequency stimulation was previously discovered in our lab at the AOB to MeA synapse of the leopard frog (*L. pipiens*), but detailed characterization had not been performed (unpublished data). In the current study, the AOT of the closely related American bullfrog (*L. Catesbeiana*) was stimulated at 1Hz, a frequency typically associated with long-term depression (LTD) in the Schaffer collateral-CA1 synapse of the mammalian hippocampus, in order to test the limits of how low a frequency is capable of inducing potentiation at the synapse (Dudek and Bear, 1992).

Repetitive 1Hz stimulation of the AOT initially produced a transient facilitation of synaptic strength, which peaked with a 20% increased amplitude at 16s, after which depression predominated, reducing the evoked response to 50% of initial amplitude by the end of a 7.5 minute train (Figure 3A). After terminating 1Hz stimulation, the strength of synaptic connection was tested every 20s. The first several minutes of testing showed a slow increase in fEPSP slope, which would be consistent with a recovery from the decrease in synaptic strength observed after 450 pulses of 1Hz stimulation (Figure 3B). Repeated measures one-way ANOVA reveals a significant effect between averaged fEPSP slopes taken during baseline measurement and following 1Hz stimulation (repeated-measures ANOVA, $F(1.81,7.24) = 39.83$, $p < 0.001$, $\varepsilon = .90$, $R^2 = .91$). Post-hoc statistical comparisons between baseline and 30 minutes post-1Hz and 60 minutes post-1Hz were made to verify the significance of the results, thus the Bonferroni adjusted α level was 0.025. One hour post-1Hz stimulation the fEPSP slope was 132 ± 8% of pre-1Hz stimulation slope and the increased synaptic strength appeared stable (post-hoc paired t-test, Bonferroni $\alpha = .025$, $df = 4$, $p \leq .001$)(Figure 3B, C).

The 50ms PPR was not significantly different from baseline following 1Hz stimulation according to paired-statistics (repeated-measures ANOVA, $F(1.27,5.08) = 3.89$, $p = .10$, $\varepsilon = .64$, $R^2 = .49$) (Figure 3D). Therefore, the increase in synaptic strength observed is consistent with changes in the sensitivity of the post-synaptic neuron, rather than pre-synaptic changes that increase probability of release.

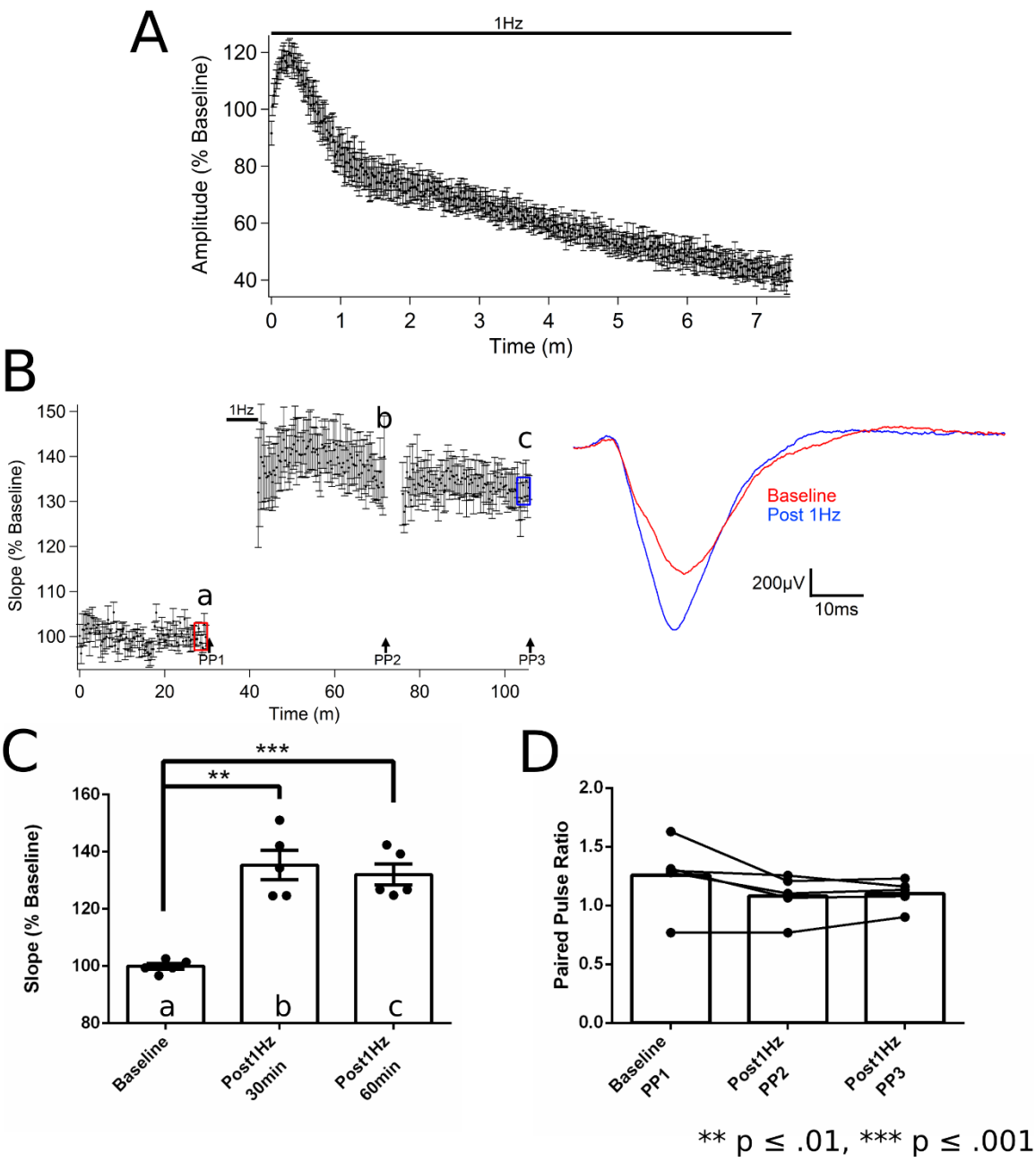

Figure 3. Stimulation frequencies as low as 1Hz are sufficient for induction of long lasting potentiation of the MeA field. (A) After a transient facilitation phase, repeated 1Hz stimulation via theta tube to the AOT results in a steady decrease in MeA fEPSP amplitude over 7.5 minutes. (B) MeA fEPSPs in response to 0.05Hz AOT stimulation are potentiated following 7.5 minutes of 1Hz stimulation delivered to the AOT. Inset shows 3-minute averages of stable pre-1Hz baseline and 1 hour post-1Hz stimulation (coloured boxes) from an example experiment. (C) fEPSP slopes remain significantly increased for over an hour post-1Hz stimulation. Lower case letters

correspond to time points in (B). (D) 50ms PPR does not change significantly following 1Hz stimulation. Time points correspond to labels in (B). Error bars indicate SEM. N = 5 (3 animals, 5 hemispheres).

A form of long-term potentiation is present at the AOB-MeA synapse. Repetitive stimulation to the AOT once every second for 7.5 minutes induced ~30% potentiation that lasted for an hour at minimum. With no significant change to 50ms PPR, the long-lasting increase in synaptic strength is consistent with post-synaptic changes. There was also no evidence for expression of post-tetanic potentiation (PTP) following the termination of 1Hz stimulation, which would have manifested as a transient increase in synaptic strength. PTP is a well-documented phenomenon of pre-synaptic enhancement that involves a temporary increase in release probability, the early phase of which is associated with a rise in pre-synaptic $[Ca^{++}]_i$ levels (Delaney et al., 1989; Zucker and Regehr, 2002). Its absence along with unchanged PPR following 1Hz stimulation suggests that this stimulation may not be frequent enough to accumulate enough Ca^{++} in the pre-synaptic terminal to induce pre-synaptic enhancement. Given that facilitation was observed during 50ms paired-pulses, repeated stimulation of higher frequencies may be better suited to induce potentiation in the pre-synapse if it is also possible at this synapse.

3.2 5Hz tetanus potentiates AOB to MeA synapse

Following the observation that several minutes of 1Hz stimulation produced potentiation lasting longer than 1 hour, the response to sets of 5Hz tetani was explored. Sustained stimulation of the AOT at 5Hz resulted in a pronounced depression of the fEPSP, therefore five 5s trains of 5Hz (25 APs each) stimulation were delivered at 15s intervals to allow for recovery from depression between bouts of stimulation. Bursts of 5Hz stimulation to the AOT potentiated the MeA fEPSP to subsequent stimuli delivered to the tract at 0.05Hz. In contrast to the response to 1Hz, there was often a transient enhancement following 5Hz tetani and potentially a lasting contribution of the pre-synapse to the observed LTP.

Following 5Hz tetanus, 5 sets of paired stimuli (50ms ISI) were delivered at intervals of 1 minute to test for effects that 5Hz stimulation might have on release. The strength of the synapse was then tested every 20s. Testing synaptic strength 4 minutes after the 5Hz trains revealed that unlike prolonged 1Hz stimulation (7.5 minutes, 450 pulses), comparatively brief sets of 5Hz tetani induced PTP that decayed approximately exponentially with a tau of 9.4 minutes (Figure 4A). Thus 5Hz tetanus produced a pronounced transient increase in synaptic strength at the AOB-MeA synapse. While the tau was quite long, the corresponding decrease in PPR shown in Figure 4C suggested the transient enhancement might be pre-synaptic PTP. Once PTP wore off, within 35 minutes of tetanus, fEPSP slope reached a stable long-term potentiated state.

Additional 5Hz stimulation, 40 minutes after the first set of tetani yielded further increase in fEPSP slope that was stable over an hour later. Once again, PTP was observed following the tetanus. Furthermore, PTP did not appear to be occluded as it supplemented the stable potentiation resulting from the first tetanus, suggesting that the mechanisms expressing the stable LTP do not overlap substantially with those underlying the pre-synaptic PTP. The final three minutes of the recording pre-tetanus were averaged for comparison to periods 30 minutes post initial 5Hz stimulation and 60 minutes after the second set of 5Hz trains (Figure 4B). Repeated-measures ANOVA confirmed that 5Hz conditioning had a significant effect at these time points (repeated-measures ANOVA, $F(1.31,9.13) = 26.98$, $p < 0.001$, $\varepsilon = .44$, $R^2 = .79$). Increases to 131% and 142% of baseline were found at each time point respectively, both significantly different from pre-tetanus (post-hoc paired t-tests, Bonferroni $\alpha = .017$, $df = 7$, $p < .0005$, $p < .005$). The increase in slope from 30 minutes after the first set of 5Hz tetani to 60 minutes after the second set of 5Hz tetani was also significant (post-hoc paired t-tests, Bonferroni $\alpha = .017$, $df = 7$, $p < .017$).

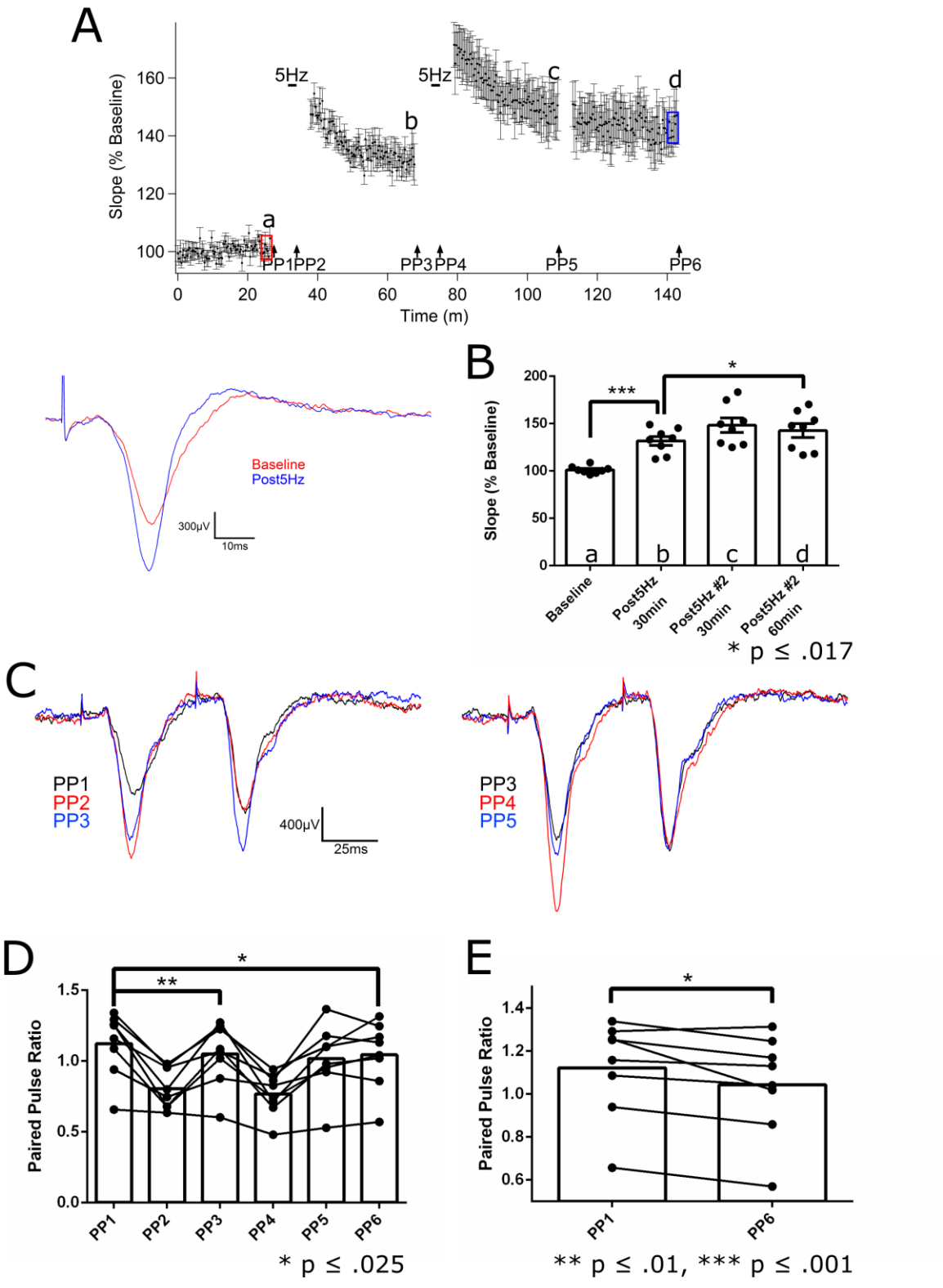

Figure 4. 5Hz stimulation induces long-term potentiation and a reduction in PPR at AOB to MeA synapse. Baseline fEPSPs in the MeA in response to 0.05Hz AOT stimulation were

recorded before and after tetanus with 50ms ISI paired-pulse testing between regular testing periods. (A) 5Hz stimulation (bar) delivered as 3 x 25 pulse tetani at 15s intervals causes potentiation of the MeA fEPSPs, with an additional set of 5Hz tetani (bar) leading to further potentiation that persists for longer than an hour. Inset shows 3-minute averages of stable pre-tetanus baseline and 30 minutes after initial 5Hz stimulation from an example experiment. (B) Averages of fEPSP slope over three minutes were taken pre-5Hz and at the end of each 0.05Hz testing period in (A) as annotated by lower case letters and used for paired statistical comparisons. (C) PP1-6 each correspond to sets of 5 paired-pulses delivered at time points labeled in (A). Averages of repeated paired-pulses from an example experiment showing before (PP1, PP3), 20s after (PP2, PP4) and 30m after (PP3, PP5) 5Hz stimulation. (D, E) 50ms PPR is decreased by 5Hz tetanus and remains lower than pre-tetanus PPR for an hour. Error bars indicate SEM. N = 8 (4 animals, 8 hemispheres).

The potentiation induced by 5Hz stimulation was accompanied by a decrease in 50ms PPR (Figure 4D). This was most apparent immediately following (PP1, first of five pairings started within 20s) the first set of 5Hz tetani, when PPR decreased to 0.804 ± 0.14 from a pre-tetanus PPR of 1.12 ± 0.23. The shifts from paired-pulse facilitation to depression after tetanus are well illustrated by PP2 and PP4, immediately after the first and second sets of 5Hz tetani respectively (Figure 4C). Repeated-measures ANOVA conducted across all of the time-points at which PPR was measured reveals a significant effect of 5Hz tetanus on PPR (repeated-measures ANOVA, $F(2.02,14.16) = 19.62$, $p < 0.001$, $\varepsilon = .40$, $R^2 = .74$). At 30 minutes post-tetanus the initial decrease in PPR was mostly reverted (1.05 ± 0.23), but remained statistically different from pre-tetanus PPR according to post-hoc paired single-comparison statistics (post-hoc paired t-test, Bonferroni $\alpha = .025$, $df = 7$, $p < .01$). This transient, large decrease in PPR corresponds to the transient PTP observed for the first few minutes of synaptic strength testing post-tetanus, which is consistent with the hypothesis that the PTP is due to pre-synaptic mechanisms (Figure 4A).

The pattern of an initial decrease in PPR below 1.0 followed by recovery to greater than 1.0 was repeated after the second set of tetani and the decrease in PPR relative to pre-tetanus was maintained over an hour later at 1.04 ± 0.24 (down from 1.12

± 0.23, PP1 vs PP6) (post-hoc paired t-test, Bonferroni $\alpha = .025$, $p < .025$). Interestingly, the stable PPR following the second set of 5Hz tetani was no lower than after the first set of 5Hz tetani despite the fEPSP being significantly more potentiated after the second set (Figure 4B, D). This suggested that while there may be some pre-synaptic component of the LTP, it became saturated following the first bout of 5Hz stimulation and did not contribute to the further increase in fEPSP strength induced by the second set of tetani.

Sets of 5Hz tetani, like repeated 1Hz stimulation, induced LTP at the AOB-MeA synapse that was stable for over one hour. It was found that unlike 1Hz stimulation, 5Hz tetanus induces a transient PTP and results in a long-term decrease in PPR. Taken together these implicate both a pronounced short-term pre-synaptic facilitation and a long-term pre-synaptic component of LTP, possibly due to increased probability of release. However, the long-term change in PPR was small and did not increase with additional 5Hz tetanus after one set, which suggests a primarily post-synaptic expression of LTP.

3.3 NMDAR antagonist AP5 does not block induction or expression of 5Hz tetani induced LTP

NMDA glutamate receptor channels have been implicated in many forms of post-synaptic LTP throughout the brain, including in the amygdala (Shin et al., 2010). Although the best studied examples of NMDAR dependent LTP are induced by high-frequency stimulation (> 10Hz), a case of 1Hz induction in the hippocampal CA1 region has been reported involving 1Hz stimulation alternating between converging inputs from CA3 and medial septal fibres. This LTP is dependent on NMDARs and insensitive to blockade of both nicotinic and muscarinic acetylcholine receptors with mecamylamine and scopolamine respectively (Habib and Dringenberg, 2009). In the present study, sets of 5Hz tetani induced LTP at the AOB-MeA synapse and the data support a predominantly post-synaptic locus of expression, so the NMDAR seemed a likely candidate for induction. The NMDAR antagonist AP5 was bath-applied before 5Hz tetanus to determine whether NMDAR receptors are required for the induction or

expression of LTP at this synapse; the data obtained do not support their involvement in either.

Bath application of 100μM AP5 resulted in decreased amplitude and slope of the MeA fEPSP when tested at 0.05Hz (Figure 5A). The decrease in slope was 24.5 ± 11.2% after 15 minutes of application. Repeated-measures ANOVA revealed that the treatments of AP5 application and 5Hz stimulation had a significant effect on fEPSP slope (repeated-measures ANOVA, $F(1.731,5.194) = 22.52$, $p < 0.005$, $\varepsilon = .58$, $R^2 = .88$). Stimulating the AOT with 5Hz tetani following AP5 application resulted in a PTP that decayed with a tau of 3.5 minutes to 127 ± 11% of fEPSP slope in the presence of AP5 pre-5Hz tetani (post-hoc paired t-test, Bonferroni $\alpha = .025$, $df = 3$, $p < .05$)(Figure 5B).

Washing out AP5 for 30 minutes revealed further potentiation, reaching 136 ± 21% of pre-AP5 slope (post-hoc paired t-test, Bonferroni $\alpha = .025$, $df = 3$, $p < .02$). The increase in slope unmasked by wash-out closely corresponded to the decrease in slope produced by application of AP5, suggesting the contribution of NMDARs to the fEPSP was consistent before and after 5Hz stimulation (Figure 5C). The fact that the unmasked portion of the fEPSP is not greater than the portion initially blocked by AP5 suggests LTP is not due to an increased sensitivity and/or number of NMDARs at the synapse. These data show that AP5 application does not prevent 5Hz induction or expression of LTP at AOB-MeA synapse, thus the mechanisms responsible are NMDAR-independent despite the large contribution of the receptor to the basal fEPSP.

PPR was measured at time points indicated in Figure 5A to determine whether AP5 interferes with the PPR decrease previously observed after induction of LTP by 5Hz stimulation (Figure 5D). Repeated-measures ANOVA revealed that AP5 application and 5Hz tetanus had a significant effect on PPR (repeated-measures ANOVA, $F(1.20,3.60) = 14.20$, $p < 0.05$, $\varepsilon = .40$, $R^2 = .83$). Following drug application there was a minor trend of increased PPR over pre-AP5 PPR but the difference did not reach statistical significance (post-hoc paired t-test, Bonferroni $\alpha = .017$, $p > .20$). The long-term potentiation of singular fEPSPs by 5Hz tetanus in the presence of 100μM AP5 was accompanied by a

significant decrease in PPR (post-hoc paired t-test, Bonferroni $\alpha = .017$, $p < .015$). After 30 minutes of drug wash-out, PPR reached a ratio of 1.15 ± 0.08, significantly reduced from pre-AP5 pre-tetanus PPR values ($1.58 \pm .13$) (post-hoc paired t-test, Bonferroni $\alpha = .017$,$df = 3$, $p < .0005$).

In light of the (statistically insignificant) trend of increased PPR in AP5, I investigated whether antagonism of NMDARs alone can impact pre-synaptic release probability by testing 50ms PPR before and after 100µM AP5 application. Data from four experiments in which AP5 was bath-applied for 30 minutes followed by 30 minutes of wash-out were combined with the pre-tetanus data from experiments presented in Figure 5D. Again, there was an increase in PPR in the presence of 100µM AP5, and with the added preparations, the effect was determined to be significant according to paired-comparison two-tailed statistics (post-hoc paired t-test, Bonferroni $\alpha = .025$, $df = 7$, $p < .02$) (Figure 5E). Unfortunately, removal of AP5 did not significantly reduce PPR (post-hoc paired t-test, Bonferroni $\alpha = .025$, $df = 7$, $p = .078$). This effect on PPR suggests a possible pre-synaptic NMDAR effect which is discussed later in this thesis.

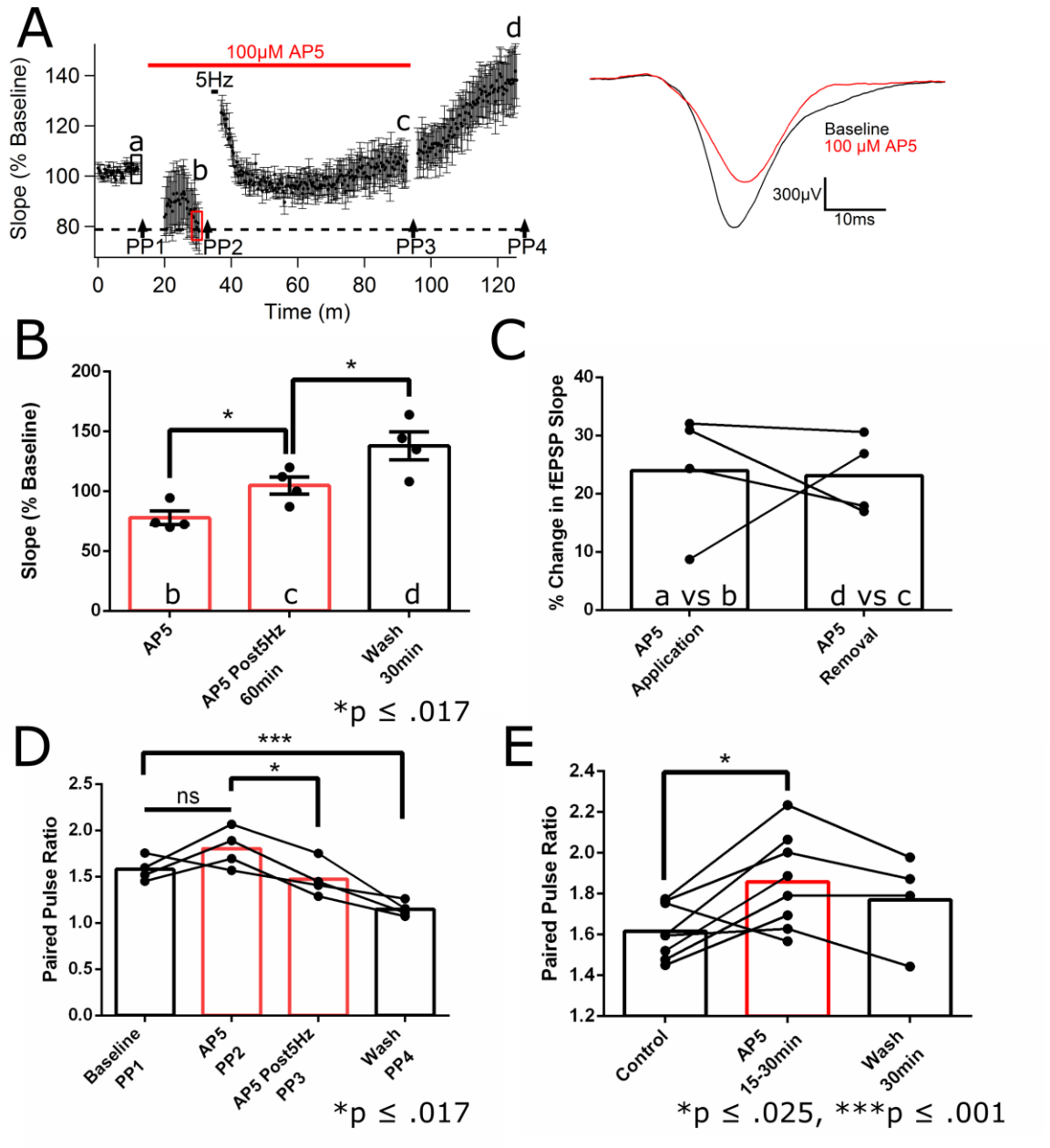

Figure 5. NMDAR antagonist AP5 inhibits MeA fEPSPs but fails to prevent LTP induction by 5Hz tetani. MeA fEPSPs in response to 0.05Hz AOT stimulation were recorded before and during AP5 application, after 5Hz tetani and following AP5 removal. (A) Following 15 minutes of bath application of 100µM AP5, MeA field is reduced in size. 5Hz tetanic stimulation increases fEPSP slope in the presence of AP5 and wash-out leads to further increase. Inset shows 3-minute averages of stable pre-AP5 baseline and AP5 fEPSPs from an example experiment. (B) Final 3-minute averages of slope are significantly different across AP5, post-5Hz and wash-out conditions. (C) Change in fEPSP slope at application and removal of AP5 is similar before and

after 5Hz stimulation. (D) AP5 does not prevent 5Hz induced decrease in PPR. Time points correspond to labels in (B). (E) Four additional experiments (2 animals, 4 hemispheres) testing for effect of 100μM AP5 alone on PPR were performed and data was combined with pre-tetanus PPRs shown in (D). Error bars indicate SEM. N = 4 (3 animals, 4 hemispheres).

Antagonism of NMDARs with 100μM AP5 was found to block a substantial fraction of the MeA fEPSP. However, despite their large contribution to resting synaptic strength, NMDARs were not required for induction or expression of LTP at the AOB-MeA synapse, as both were insensitive to presence of AP5 during and after 5Hz tetanus. AP5 increased PPR independent of 5Hz tetanus and LTP, suggesting that NMDARs may increase pre-synaptic release probability or alter the expression of paired-pulse facilitation (McGuinness et al., 2010). 5Hz tetani decreased PPR when delivered in the presence of AP5, as it does in the absence of AP5. In these experiments, the decrease in PPR caused by 5Hz tetanus was greater than the decrease observed in initial experiments (Figure 4D), suggesting there might be greater change in pre-synaptic release than we previously observed.

3.4 KAR antagonist UBP310 partially blocks expression of LTP, but does not prevent its induction by 5Hz tetani

Next I hypothesized that glutamatergic KARs were a key mechanism in the 5Hz tetanus inducible AOB-MeA LTP. These receptors, particularly those containing the GluK1 (previously GluR5) subunit, have been implicated in the low-frequency stimulation induced pre-synaptic LTP in the rodent amygdala (Li et al., 2001; Shin et al., 2010). Our characterization of the AOB-MeA 5Hz LTP thus far could be consistent with both pre- and post-synaptic changes and KARs are found in both locations making them potential candidates for induction and expression of LTP at this synapse (Huettner, 2003). In order to test for the involvement of KARs, the antagonist UBP310 was used. UBP310 specifically blocks KARs while sparing AMPARs and NMDARs. Though originally developed as a GluK1 subunit antagonist, UBP310 has since been found also to be a

potent antagonist of GluK2/5 heteromers, which are primarily post-synaptic and are the most abundant KAR in the CNS (Lerma, 2006; Pinheiro et al., 2013).

Pre-synaptic KARs mediate both up-regulation and down-regulation of release at different synapses in the CNS (Rodríguez-Moreno and Sihra, 2007). Therefore, before investigating the importance of KARs in LTP induction and expression, paired stimulus testing was performed on tetanus-naive tissue to measure changes in PPR elicited by application of a KAR antagonist alone. In the presence of 10μM UBP310, fEPSPs were reduced in strength relative to control (Figure 6A). Similar to AP5, UBP310 application has a significant effect on PPR, suggesting that some of the reduction in fEPSP strength may be due to decreased probability of release, although direct effects on paired-pulse facilitation are not ruled out (McGuinness et al., 2010) (Figure 6B). The pre-UBP310 50ms PPR of 1.89 ± 0.39 increased to 2.23 ± 0.28 within 30 minutes of 10μM UBP310 application, however the difference does not reach significance according to a Bonferroni adjusted paired t-test (post-hoc paired t-test, Bonferroni $\alpha = .025$, $df = 7$, $p = .028$). However, the trended change was significantly reversed following removal of the drug (post-hoc paired t-test, Bonferroni $\alpha = .025$, $df = 7$, $p < .01$) (repeated-measures ANOVA, $F(1.88,13.16) = 7.99$, $p < 0.01$, $\varepsilon = .94$, $R^2 = .53$) (Figure 6C). These data are consistent with KARs having a facilitatory role in pre-synaptic transmitter release, supplementary to any contribution they make to the post-synaptic response. Similar actions of KARs have been reported in the hippocampus, where low concentrations of kainate – thought to activate metabotropic function – can increase probability of release through PKA dependent mechanisms at mossy fibre to CA3 synapses (Rodríguez-moreno and Sihra, 2011).

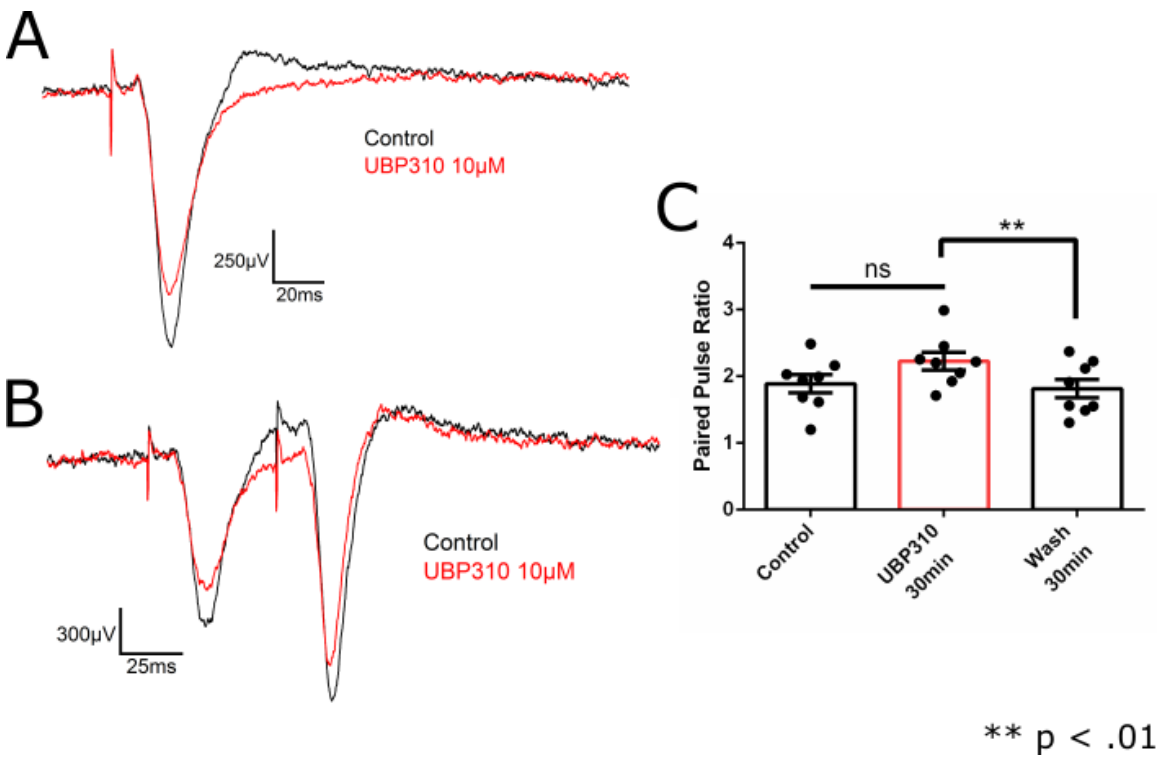

Figure 6. Antagonism of KARs by UBP310 increases PPR in the MeA. (A) Bath application of 10μM UBP310 for 30 minutes reduces the strength of AOT evoked MeA fEPSPs. Averages of 3 minutes of 0.05Hz synaptic strength testing from an example experiment are shown. (B) The decrease in MeA response to AOT stimulation is accompanied by an increased 50ms PPR. Averages of 3 pairs of 50ms ISI stimuli from an example experiment are shown. (C) The 50ms PPR is reversibly increased by 10μM UBP310. N = 8 (5 animals, 8 hemispheres).

After establishing that KARs are present at the synapse and contribute to the MeA fEPSP, 10μM UBP310 was bath-applied before 5Hz tetani to test for KAR contribution to LTP. Once synaptic strength had stabilized in UBP310, 5Hz tetani were delivered and synaptic strength testing was continued at 0.05Hz in the constant presence of UBP310 to monitor for PTP and LTP.

Bath application of 10μM UBP310 reduced fEPSP slope to 71 ± 8% of pre-UBP310 levels (Figure 7A). Sets of 5Hz tetani delivered to the AOT after 40 minutes of UBP310 application resulted in a brief PTP, which peaked at ~187% of pre-tetanus slopes in the presence of UBP310 before it decayed with a tau of 4.6 minutes. After PTP

diminished, fEPSP slope remained stably potentiated at 141 ± 20% over pre-tetanus slopes in the presence of UBP310 (post-hoc paired t-test, Bonferroni $\alpha = .017$, $df = 4$, $p < .01$) (Figure 7B). Both 5Hz tetanic stimulation and post-tetanus synaptic strength testing were performed in the presence of UBP310; therefore, the observed potentiation was both induced and expressed independent of KARs (GluK1 containing receptors or GluK2/5 heteromers).

While LTP was expressed during UBP310 application, a KAR-dependent component of the potentiation might still be masked, therefore synaptic strength was continuously tested as the drug was removed. During UBP310 wash-out the fEPSP slope increased up to 170 ± 24% of baseline, significantly greater than the potentiated fEPSP in UBP310 (post-hoc paired t-test, Bonferroni $\alpha = .017$, $df = 4$, $p < .001$). Comparison of the effect on fEPSP slope of application and removal of UBP310 reveals a trend towards a greater drug effect post-tetanus than pre-tetanus. While 42 ± 7% of the post-tetanus fEPSP was blocked by UBP310, only 29.2 ± 7.8% was blocked pre-tetanus (Figure 7C). The trend fails to reach statistical significance using paired-comparisons with this sample size; however, 5Hz tetani enhanced the percentage of fEPSP blockade by UBP310 in all but one (4/5) experiment (single paired t-test, $df = 4$, $p = .055$). A greater proportionate block/masking of the fEPSP by UBP310 post-tetanus would be consistent with KARs participating in the expression of the 5Hz tetanus-induced LTP at this synapse. LTP is not entirely dependent on these KARs as 5Hz tetani did increase fEPSP strength in the presence of UBP310, but the data are consistent with KARs contributing to enhancement of synaptic strength observed following 5Hz tetanic stimulation.

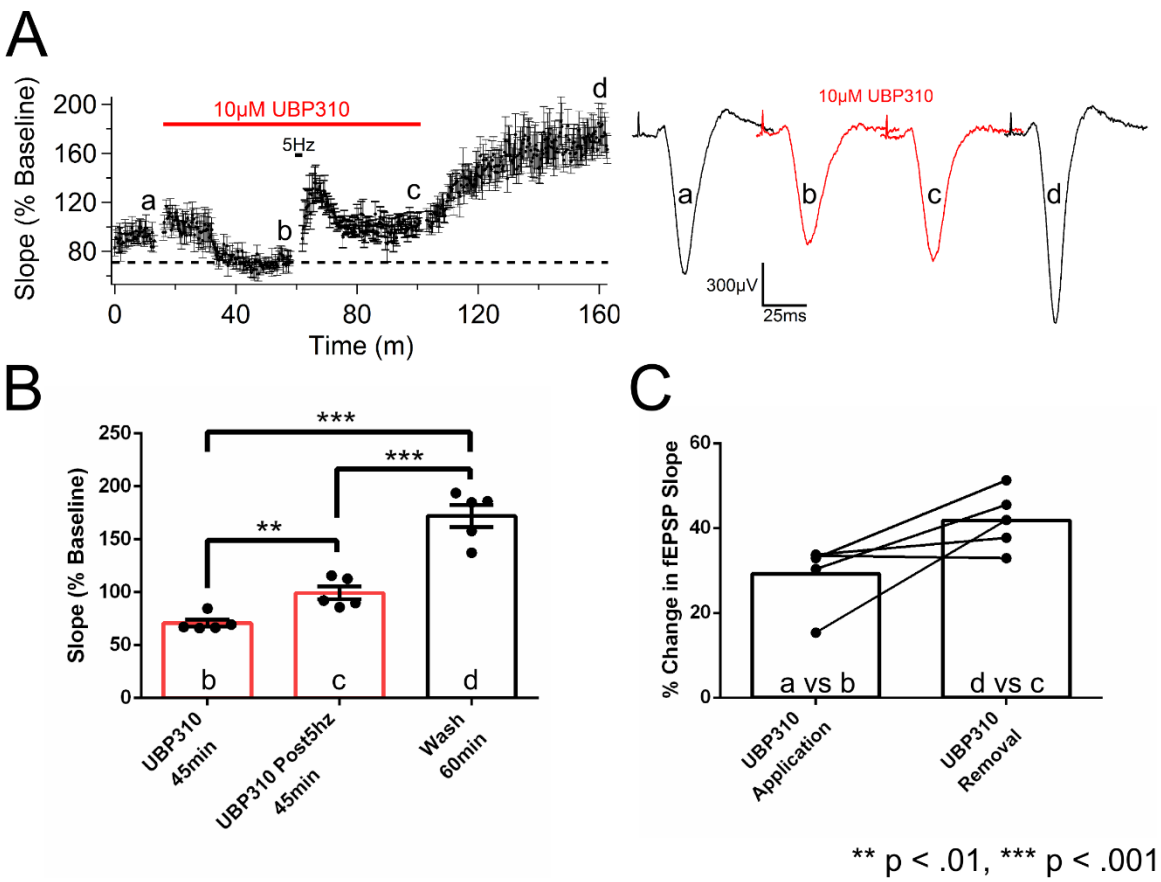

Figure 7. 5Hz LTP induction is insensitive to KAR antagonist UBP310, but expression is partially blocked. MeA fEPSPs in response to 0.05Hz AOT stimulation were recorded before and during UBP310 application, after 5Hz tetani and following UBP310 removal. (A) Bath application of 10μM UBP310 decreases fEPSP slope. Stimulation of the AOT with 5x 5Hz tetani (25 stimuli each) with 15s intervals increases fEPSP slope in the presence of UBP310 and subsequent wash-out increases slope further. Inset shows example 3-minute averages of time points corresponding to lowercase labels. (B) Slope increases following 5Hz tetani and UBP310 removal are significant according to paired-statistics. Time points correspond to labels in (A). (C) Proportion of fEPSP slope sensitive to UBP310 before and after 5Hz stimulation. Time points used to calculate changes correspond to labels in (A). N = 5 (4 animals, 5 hemispheres).

5Hz tetanic stimulation of the AOT induced LTP in the presence of UBP310, but expression was partially masked until the drug was removed. Based on these data, I hypothesized that GluK1 subunit containing and/or GluK2/5 receptors are not required

for induction of LTP, but their up-regulation contributes to the expression of LTP at the AOB-MeA synapse. Further experiments in which LTP was induced via 5Hz tetani before application of UBP310 were performed to test whether the decrease in synaptic strength following UBP310 application would be greater compared to that observed in tetanus-naive tissue.

3.5 Blocking KARs after LTP induction substantially reduces fEPSP

In order to test the effect UBP310 might have on a potentiated AOB-MeA synapse, 10μM UBP310 was bath-applied 1 hour after 5Hz tetanic stimulation to the AOT (Figure 8A). Treatments of 5Hz stimulation and UBP310 application were again found to have a significant effect on fEPSP slope (repeated-measures ANOVA, $F(2.17,10.86) = 26.73$, $p < 0.001$, $\varepsilon = .54$, $R^2 = .84$). Prior to bath application of UBP310, fEPSP slope was potentiated to 188 ± 30% of pre-tetanus baseline (post-hoc paired t-test, Bonferroni $\alpha = .017$, $df = 5$, $p < .001$). Application of UBP310 decreased fEPSP slope to 111 ± 23% of pre-tetanus baseline (post-hoc paired t-test, Bonferroni $\alpha = .017$, $df = 5$, $p < .0001$) (Figure 8B). This proportional change more closely resembles the increase in slope observed when UBP310 was removed following 5Hz tetanus than when UBP310 was applied to the tetanus-naive MeA. Here, 41.1 ± 7.1% of the fEPSP was blocked by UBP310, which is well within the margin of error of the proportion of the fEPSP masked by UBP310 when 5Hz tetani were delivered in the presence of the drug, 41.9 ± 7.1% (Figure 7C). This supports the hypothesis that KARs contribute to the expression of LTP induced by 5Hz tetanus. The drug effect was reversible as fEPSPs returned to pre-drug application slopes following wash-out, 182 ± 22% of pre-tetanus slope, significantly increased over pre-tetanus baseline (post-hoc paired t-test, Bonferroni $\alpha = .017$, $df = 5$, $p < .0005$).

As in previous experiments, PPR decreased in parallel to increases of fEPSP slope elicited by 5Hz tetanus (Figure 8C). Repeated-measures ANOVA revealed that the treatments of 5Hz tetanus and UBP310 had a significant effect on PPR (repeated-

measures ANOVA, $F(2.25,11.22) = 6.35$, $p < 0.05$, $\varepsilon = .75$, $R^2 = .56$). Prior to tetanus or UBP310 application, 50ms paired-pulse stimulation elicited strong facilitation with a PPR of 1.72 ± 0.23. Facilitation was still present following 5Hz stimulation, but PPR was significantly reduced at 1 hour post-tetanus, 1.36 ± .18 (post-hoc paired t-test, Bonferroni $\alpha = .017$, $df = 5$, $p < .01$). Application of UBP310 had the opposite effect, increasing PPR to 1.68 ± .39, significantly higher than post-tetanus pre-UBP310 levels (post-hoc paired t-test, Bonferroni $\alpha = .017$, $df = 5$, $p < .015$). Removal of UBP310 appeared to decrease PPR, however the trend was not significant to the Bonferroni adjusted α level for 3 post-hoc comparisons (post-hoc paired t-test, Bonferroni $\alpha = .017$, $df = 5$, $p = .043$).

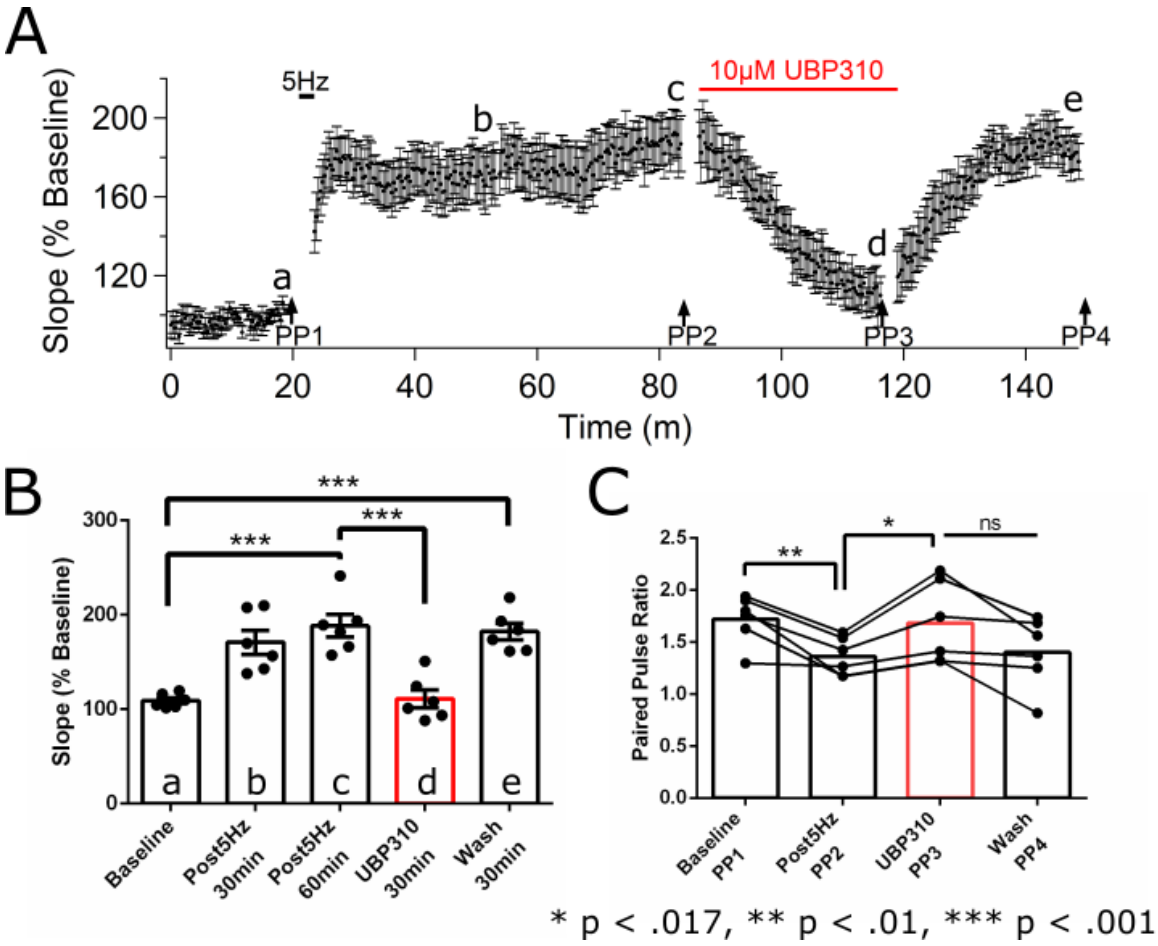

Figure 8. KAR antagonist UBP310 dramatically decreases long-term potentiated MeA field response. MeA fEPSPs in response to 0.05Hz AOT stimulation were recorded before and after 5Hz tetani and during UBP310 application and removal. Paired-pulse testing was performed

between 0.05Hz testing periods, as indicated by PP labels. (A) Bath application of 10μM UBP310 1 hour after 5Hz stimulation (bar) reversibly decreases MeA fEPSP slope. (B) 3-minute averages of the time points labeled in (A) were used for paired-comparison statistics. (C) 5Hz tetanic stimulation reduces 50ms PPR and 10μM UBP310 bath application to the tetanus-potentiated synapse increases 50ms PPR. N = 6 (5 animals, 6 hemispheres).

UBP310 application to the potentiated AOB-MeA synapse resulted in a profound decrease in fEPSP slope. Comparing Figure 8 to Figure 7, which shows the reduction of fEPSP by UBP310 applied to the tetanus-naive synapse, there was a greater effect of UBP310 on the long-term potentiated synapse. The proportion of the potentiated fEPSP blocked by UBP310 after 5Hz tetanus closely correlates with the proportion of the fEPSP masked by UBP310 when LTP was induced in the presence of the drug (see 3.4, Figure 7C). The larger effect of UBP310 on potentiated fEPSPs relative to tetanus-naive fEPSPs supports the hypothesis that KARs are involved in the expression of LTP at the AOB-MeA synapse.

The 50ms PPR was increased when UBP310 was applied to the long-term potentiated synapse, which is similar to the effect of UBP310 applied to the tetanus-naive AOB-MeA synapse (Figure 6C; Figure 8C). In both cases, the increase in PPR was approximately 20%. Regardless of the state of potentiation of the synapse, UBP310 seemed to have the same magnitude of effect on PPR despite having a variable effect on synaptic strength. This is consistent with KAR receptors not changing their influence on release probability following 5Hz tetanic stimulation. Therefore, the enhanced KAR-dependent portion of the fEPSP likely has a predominantly post-synaptic locus of expression.

Chapter 4 – Discussion

4.1 Synaptic Model

The AOB-MeA synapse contains a variety of glutamate receptors whose currents contribute to the fEPSPs recorded in the experiments presented here. Application of the NMDAR antagonist AP5 blocked ~25% of the evoked field and the KAR antagonist UBP310, selective for GluK1 subunit-containing receptors and GluK2/5 heteromers, blocked ~29%. Both of these antagonists increased PPR, consistent with some or all of their effect being due to pre-synaptic inhibition. Thus their true contribution to the post-synaptic response is difficult to ascertain. Previously, Mulligan *et al.* (2001) demonstrated that the AMPAR/KAR antagonist CNQX blocks post-synaptic response completely at this synapse, suggesting that these receptors are responsible for the majority of the observed fEPSP. When 100-150µM AP5 was applied following CNQX, no additional blockade was observed, which would be consistent with NMDAR requiring the membrane depolarization provided by other ionotropic glutamate receptors to relieve their Mg^{++} pore-block.

Repetitive 5Hz stimulation of the AOT leads to LTP of the MeA fEPSP. Induction of LTP was not prevented by the application of AP5 or UBP310 alone, ruling out NMDARs, GluK2/5 heteromers and/or GluK1 subunit containing KARs as essential to LTP induction. However, antagonism of KARs by UBP310 blocked a greater proportion (~41%) of the potentiated fEPSP than the tetanus-naive fEPSP (~29%), suggesting KARs are required for the expression of LTP. These results are consistent with increased current fluxing through UBP310 sensitive KARs during LTP expression. I propose that an increase in KARs at the synaptic membrane accounts for some, but not all, of the LTP expressed and the remaining UBP310 insensitive potentiation is due, at least in part, to an increased probability of release (Figure 9).

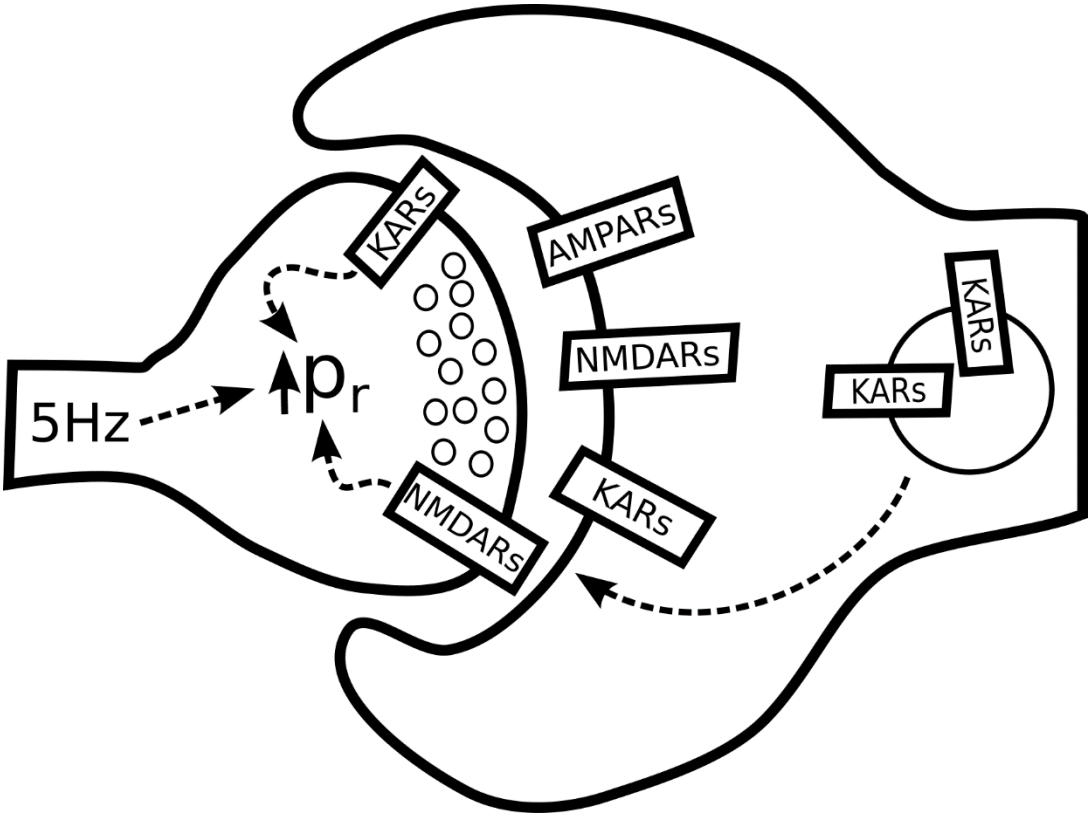

Figure 9. Hypothesized synaptic model of LTP at the AOB-MeA synapse. Following 5Hz stimulation, pre-synaptic probability of release (p_r) is increased. Effects of AP5 and UBP310 on PPR point to NMDARs and KARs tonically increasing probability of release. Post-synaptic LTP is expressed by increased KAR trafficking to the post-synaptic membrane. The mechanisms of induction of neither pre- nor post-synaptic LTP are known.

4.1.1 Post-tetanic potentiation

Stimulation of the AOT with 5Hz tetani, but not a 1Hz train (Figure 2B), induces PTP at this synapse that lasts ~20-25 minutes (Figure 3A). PPR measurements taken between 20s and 5 minutes after termination of 5Hz tetani are significantly decreased relative to pre-tetanus PPRs and PPRs at 30 minutes post-tetanus. This transient reduction of PPR is consistent with the AOB-MeA PTP being at least in part due to increased probability of release. I propose that the mechanisms underlying the increased release

probability of PTP and LTP may differ due to the lack of occlusion of PTP observed when a second set of 5Hz tetani are delivered to an already potentiated synapse (Figure 4A).

Induction of this short-term plasticity phenomenon is dependent on $[Ca^{++}]_i$ buildup caused by tetanic bursts of APs. In crayfish the degree of enhancement of the post-synaptic response following termination of tetanus decays at the same rate as pre-synaptic $[Ca^{++}]_i$, suggesting that the temporary increase in vesicular release is tied to Ca^{++} (Delaney et al., 1989). However, studies in rodents have demonstrated cases where PTP-enhanced glutamate release from CNS neurons continues after tetanus elevated $[Ca^{++}]_i$ has already decayed to basal levels (Regehr et al., 1994; Brager et al., 2003). Thus in at least some synapses, Ca^{++} is acting on Ca^{++} sensitive kinases such as PKC (Brager et al., 2003; Fioravante et al., 2014), which have vesicular release machinery proteins like Munc18-1 as substrates (Genç et al., 2014), rather than directly stimulating release. Typically PTP is reported to persist over shorter timeframes, from tens or hundreds of seconds to several minutes, than in the present study (Zucker and Regehr, 2002; Fioravante and Regehr, 2011). Either $[Ca^{++}]_i$ remains elevated in AOB mitral cell terminals for > 15 minutes following completion of 5Hz tetani, or release-associated proteins are transiently phosphorylated and take several minutes to be dephosphorylated after $[Ca^{++}]_i$ has returned to resting levels.

4.1.2 Pre-synaptic vs Post-synaptic expression

Recently, GluK2-containing KARs were found to be trafficked to the post-synaptic membrane of dissociated hippocampal neurons following weak stimulation by a low concentration of agonist (10µM kainate; González-González and Henley, 2013). Kainate stimulated metabotropic action of KARs lead to phosphorylation of endosome-bound GluK2 through protein kinase C (PKC). Newly phosphorylated KARs were then trafficked from the dendritic shaft to the spine head where they inserted into the post-synaptic membrane. This is analogous to the well characterized Ca^{++} / calmodulin-

dependent protein kinase II (CamKII) dependent trafficking of AMPARs that produces LTP at the CA3-CA1 hippocampal pyramidal neuron synapses (Malinow et al., 1988, 1989; Mayford et al., 1995; Byth, 2014). G-proteins, phospholipase C (PLC), release of Ca^{++} from intracellular stores and PKC were all required for KAR trafficking; inhibition of any one of these components prevented the effects of kainate on KAR recycling. PKC activated by group 1 mGluRs can also increase current fluxed by GluK2/5 receptors, as observed by Rojas et al. (2013). In the present study, a potent antagonist of GluK2/5 receptors — the most abundant primarily post-synaptic KAR in the CNS (Lerma, 2006) — was found to have a stronger effect on long-term potentiated synapses than it had on tetanus-naive synapses. Because the effect of UBP310 on PPR was not increased after induction of LTP, I hypothesize that part of the potentiation observed following 5Hz tetanic stimulation is due to increased presence of GluK2/5 receptors at the post-synaptic membrane.

Expression of LTP was not completely blocked by UBP310, suggesting that a combination of increased pre-synaptic release probability (supported by the decrease in PPR) and other post-synaptic changes (insensitive to AP5 or UBP310) accounts for the remaining potentiation (Figure 7). Supposing that there are more GluK2/5 containing receptors at the post-synaptic membrane following LTP induction, additional neurotransmitter release may be able to account for a substantial portion of the remaining potentiation observed in the presence of UBP310. Increased glutamate release would lead to additional activation of – and cation flux through – all post-synaptic glutamate receptors, including the inflated population of GluK2/5 receptors. Unlike coincident post-synaptic changes which would be additive, parallel pre- and post-synaptic changes should be multiplicative. Enhanced release coupled with increased numbers of receptors available on the post-synaptic membrane will theoretically cause a larger potentiation of the post-synaptic response than the sum of their parts. For this reason I suspect that most of the LTP observed can be attributed to both the enhanced probability of release and the increased GluK2/5 population.

In order to check whether this idea is supported by my data, I performed some simple estimations using the data presented in results sections 3.4 and 3.5. On average, UBP310 blocked ~30% of the pre-tetanus fEPSP and ~42% of the post-tetanus fEPSP (Figure 7C; Figure 8B). Theoretical receptor populations based on these values are estimated and presented graphically in Figure 10.

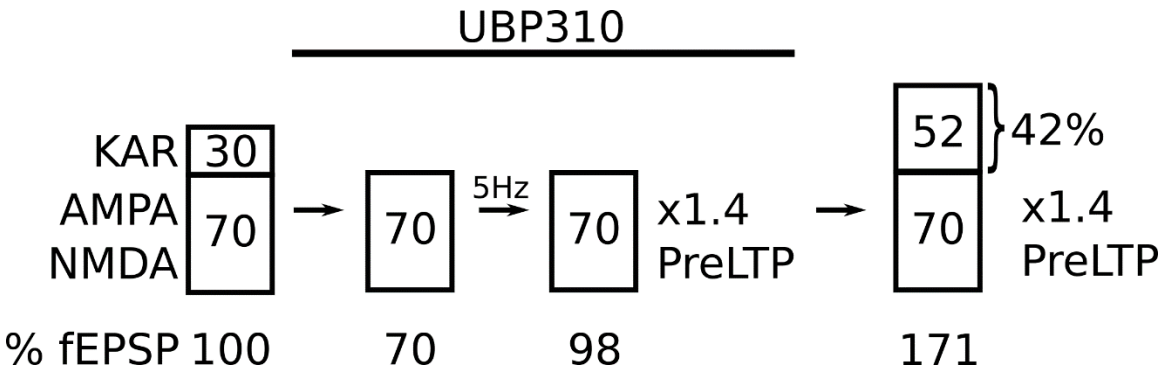

Figure 10. Post-synaptic KAR receptor population increase in parallel with UBP310-insensitive pre-LTP can theoretically account for a majority of the observed LTP. Theoretical ionotropic glutamate receptor populations, estimated based on % fEPSP block by UBP310, are presented in boxes. Normalized fEPSP strength estimations at each stage of the experiment based on the available glutamate receptors are listed below. A 1.4-fold LTP (hypothesized to be pre-synaptic) is induced in the presence of UBP310, so enhanced release is only interacting with the non-KAR fraction of post-synaptic glutamate receptors. Upon removal of UBP310, ~42% of the final fEPSP is unblocked which is interpreted here as an increased number of KARs at the post-synaptic membrane. Interaction of the inflated glutamate receptor population with enhanced release produces a theoretical normalized fEPSP strength of 171%.

Assuming other receptor populations (*e.g.* AMPARs and NMDARs) remain the same, the population of UBP310-sensitive KARs (*e.g.* GluK2/5) is projected to increase by ~75% in order to account for ~12% more of the fEPSP. This increase would bring the theoretical glutamate receptor population to ~122% of pre-tetanus levels, thus potentiating the post-synaptic response 1.22 fold. However, while those KARs are blocked in the persistent presence of UBP310, fEPSPs were potentiated ~1.4 fold by 5Hz tetani. Following the assumption that this increase is entirely pre-synaptic and will

combine multiplicatively with post-synaptic changes (x1.22), I calculated the theoretical total LTP that should be revealed by UBP310 removal. The product of the pre-synaptic LTP (x1.4) with the theoretical post-synaptic receptor population increase (x1.22) comes to an estimated 1.72-fold LTP over the pre-drug tetanus-naive fEPSP. This is well within the margin of error of the experimental total LTP observed following removal of UBP310 in experiments where 5Hz tetani were delivered in the presence of UBP310 (170 ± 24%; Figure 7).

A pitfall of the calculation above is that it does not account for the unknown proportion of fEPSP reduction by UBP310 that results from a decrease in probability of release, which is implied by the increase in PPR in the presence of UBP310. Antagonism of pre-synaptic UBP310-sensitive KARs (*e.g.* GluK1-containing) receptors likely accounts for an unknown proportion of the ~30% decrease in fEPSP pre-tetanus caused by UBP310 , which means the theoretical receptor population increase that is used to calculate total theoretical LTP above is over-estimated. Fortunately for the proposed model, the theoretical LTP (~172%) is well within the margins of error of experimental LTP (170 ± 24%) when direct effects of UBP310 on release probability are unaccounted for. Even in a scenario in which UBP310 blocks enough release that the glutamate receptor population increase was over-estimated by a factor of 2 (*e.g.* final receptor population is ~111% of pre-tetanus), the theoretical LTP would be calculated at ~156%, still within two standard deviations (a range that should encompass 68% of replications) of experimental results.

Another consideration that must be addressed is the possibility that the pre-synaptic effect of UBP310 might be altered by 5Hz tetani, which would invalidate the assumptions upon which the calculations depicted in Figure 10 are based. While it cannot be ruled out entirely, there is evidence from the PPR results that suggests the contribution of KARs in the pre-synapse are unchanged. Whether UBP310 is applied before or after 5Hz tetanus, does not change the effect it has on PPR. Comparison of the data presented in Figure 6C and Figure 8C shows application of UBP310 to tetanus-naive synapses and long-term potentiated synapses alike results in a 20% increase in PPR. Thus, LTP

induction does not alter the pre-synaptic effect of UBP310 on release probability. If the measurable pre-synaptic effect of UBP310 remains constant, attributing the increased efficacy of fEPSP block by UBP310 post-tetanus to post-synaptic changes becomes more appropriate. This is because the unknown element in the calculation discussed above would primarily affect initial values rather than being dynamic.

4.1.3 Potential post-synaptic induction mechanisms

In González-González and Henley's (2013) experiments G-proteins, PLC and intracellular Ca^{++} release were all required to drive PKC, which is the key downstream mechanism responsible for increasing the population of KARs at the membrane following KAR stimulation. Since antagonism of KARs (both GluK1-containing receptors and GluK2/5 heteromers) via UBP310 does not prevent LTP induction at the AOB-MeA synapse, there must be another causal agent or agents activated by 5Hz stimulation that is/are capable of driving the downstream expression of LTP. If PKC is involved in the enhancement of the post-synaptic KAR response in the AOB-MeA synapse, any channels or proteins upstream of PKC that could lead to its activation are candidate LTP induction mechanisms at this synapse. I propose that from the glutamate receptors present at the synapse, NMDARs, GluK2/5 KARs, and possibly group 1 mGluRs may all be capable of enabling PKC activation in response to 5Hz tetani. Thus blockade of one glutamate receptor type alone will not prevent LTP induction.

In the case of the aforementioned study on the membrane insertion of GluK2-containing KARs, the post-synaptic KARs signalled via Gq alpha subunit proteins (González-González and Henley, 2013). Metabotropic action of KARs was driven by bath application of 10µM kainate for 3 minutes, whereas LTP in the present study was induced by 25s of 5Hz stimulation delivered over 2 minutes. The key difference between our study and González-González and Henley was that we non-specifically activated all glutamate receptors. Several paradigms of low-frequency (< 10Hz) repetitive/tetanic stimulation of this sort have been shown to be sufficient to induce NMDAR-, KAR- and

group 1 mGluR-dependent forms of LTP (Habib and Dringenberg, 2010a, 2010b). Therefore, the 5Hz tetanic stimulation utilized in this study could be sufficient to induce LTP dependent on any of these receptors, given the right circumstances.

Group 1 mGluRs and KARs have been found to cooperate in the induction of input timing dependent LTP in the rat lateral amygdala by repetitively pairing stimulation of cortical and thalamic inputs 15ms apart at 1Hz (Cho et al., 2011). Activation of both mGluRs and KARs, either by specific agonists — DHPG and ATPA respectively — or synaptic stimulation — when not blocked by MPEP or UBP302 —, were both required to induce LTP in the lateral amygdala neurons. Since inclusion of the Ca^{++} chelator BAPTA in the recording pipette also prevented LTP induction, the authors hypothesized that post-synaptic $[Ca^{++}]_i$ rise was a key factor and that both receptors were required to meet the necessary threshold. Group 1 mGluRs indirectly leading to Ca^{++} release from internal stores through the second messenger inositol triphosphate (IP_3) and KARs, which they assumed to be Ca^{++} permeable GluK1-containing receptors, both contributed to LTP induction. A more recent study by Pinheiro et al. (2013) revealed that GluK2/5 heteromers are also sensitive to UBP302 and ATPA thus the LTP observed by Cho et al. (2011) could have been dependent on a wider array of KARs.

For KARs and group 1 mGluRs acting metabotropically, the pathway to activation of PKC is two-fold once an active Gq alpha subunit binds with the enzyme PLC. First, PLC hydrolyzes phosphatidylinositol 4,5-bisphosphate (PIP_2) into diacyl glycerol (DAG) and IP_3. Then, DAG directly interacts with PKC and IP_3 releases Ca^{++} from the smooth endoplasmic reticulum, indirectly stimulating PKC (Berridge, 1993; Fioravante et al., 2014). Acting as ionotropic receptors, NMDARs can contribute to the activation of PKC via fluxing Ca^{++} (Rodríguez-Durán and Escobar, 2014). Though unlike KARs and mGluRs, NMDARs require sufficient depolarization of the post-synaptic membrane in order to open, which low stimulation frequency paradigms like the 5Hz tetani used in the present study are not typically thought to provide. This is because at higher frequencies (*e.g.* 100Hz) APs arrive at terminals close enough in time to allow temporal summation of EPSPs, depolarizing the post-synaptic membrane enough to

relieve the Mg^{++} pore blockade of NMDARs (Rosenzweig et al., 1997). However, some characteristics of the bullfrog forebrain preparation might improve the conditions for activation of NMDARs, as evidenced by their large contribution to single stimulation fEPSPs (Figure 5A, B), making their substantial (~23%) contribution, as measured by the effect of AP5, to the resting fEPSP at this synapse viable.

A few characteristics of the bullfrog forebrain preparation used in this study spread the stimulation of the MeA out temporally, such that APs generated at the origin of the AOT do not all reach their terminals at the same time. In the present study, the tract was stimulated approximately 1.5-2mm away from its termination in the MeA. Axons of the tract keep to a fairly tight bundle, but a combination of their arcing trajectory along the lateral wall and their fanning at the terminal field of the MeA provide the possibility of differences in length (Mulligan et al., 2001). This combined with any potential differences in conduction velocity between axons due to different axonal diameters (Seidl, 2013) leads to a long lasting axon volley by the time APs reach the terminal field. The volley spans ~7ms and given AMPAR excitatory post-synaptic current (EPSC) durations of ~20ms (Andrásfalvy and Magee, 2004) there is a strong likelihood that spatio-temporal summation would occur at any MeA neurons that receive inputs from multiple terminals of the AOT (Figure 2B). Each single stimulation to the tract could result in repeated release events on-to single neurons in rapid succession, simulating a higher frequency stimulation train than that being delivered to the AOT. This might allow for glutamate release to coincide with post-synaptic depolarization, fulfilling NMDARs conditions for channel opening. I hypothesize that this scenario may add to the large contribution by NMDARs (24.5 ± 11.2%) to single MeA fEPSPs, whether it be occurring pre-synaptically or post-synaptically (Figure 5A).

4.1.4 Pre-synaptic receptors and signalling

4.1.4.1 NMDA receptors

In the present study, bath application of AP5 decreases the strength of fEPSPs by ~25% (Figure 5A, B). AP5 also increases the 50ms PPR in the MeA (Figure 5E), which would be consistent with a decrease in the probability of neurotransmitter release contributing to the reduction in synaptic strength observed (Delaney et al., 1989; Debanne et al., 1996; Dobrunz and Stevens, 1997; Dobrunz et al., 1997; Zucker and Regehr, 2002). At synapses with high release probability, repeated stimulation at short intervals can deplete the readily releasable pool of vesicles, resulting in less neurotransmitter being released into the synaptic cleft by the second AP of a pair (Zucker and Regehr, 2002). When PPR increases, as it does in response to AP5, it may be due to reduced release probability allowing for more vesicles to be available for release by the second AP. This suggests that NMDARs are tonically regulating release from AOB mitral cell terminals.

Tonic release facilitation by NMDARs has been reported previously in rat entorhinal cortical neurons, where blockade of NMDARs with AP5 decreases the frequency of spontaneously occurring miniature excitatory post-synaptic currents (mEPSCs) (Berretta and Jones, 1996). Selective blockade of post-synaptic NMDAR conductance by inclusion of MK-801 (a non-competitive, use-dependent, pore-blocker) in the recording pipette had no effect on mEPSC frequency. Thus, the effect of AP5 on mEPSC frequency was due to antagonism of receptors on the pre-synaptic terminal, rather than preventing ion flux through post-synaptic NMDARs. Pre-synaptic NMDARs have also been found to facilitate glutamate release in the dorsal motor nucleus of mouse vagus nerve (Bach and Smith, 2012). The frequency of dorsal motor nucleus mEPSCs was increased by bath application of NMDA and decreased by AP5. Additionally, AP5 increased the PPR between dorsal motor nuclei EPSCs evoked by stimulation to the nucleus of the solitary tract (Bach and Smith, 2012). These studies together set a precedent for NMDARs facilitating glutamate release and are consistent with my interpretation that AP5 reduces probability of release at the AOB-MeA synapse in addition to any post-synaptic effects it might have.

How NMDARs tonically increase release from pre-synaptic terminals has not yet been well characterized. Presumably NMDAR channels must either be able to open at resting membrane potentials and flux cations, or perform some metabotropic function independent of channel opening. Studies in support of both of these modes of action of NMDARs are discussed below.

It has been demonstrated that post-synaptic NMDARs in the neocortex of the rat can flux at resting membrane potentials in response to asynchronous release (Espinosa and Kavalali, 2009). Approximately ~20% of the charge transfer (area) of spontaneously occurring mEPSCs recorded at -67mV in layer IV neocortical neurons were blocked by application of the antagonist AP5. The resting mEPSC NMDAR component was also resilient to decreases in post-synaptic response caused by partial block of AMPARs, indicating that the result was not entirely due to local depolarizations being sufficient to relieve Mg^{++} block of NMDAR channels. Based on these findings, Espinosa and Kavalali (2009) postulated that Mg^{++} block at resting potential with physiological levels of $[Mg^{++}]_i$ may not be absolute and some NMDARs are capable of ion flux upon agonist binding at resting conditions. Thus, NMDARs could feasibly flux Ca^{++} into the pre-synapse in a non-activity-dependent manner and tonically facilitate release by increasing $[Ca^{++}]_i$.

Alternatively, NMDARs may also affect neurotransmitter release through a metabotropic function independent of channel opening and direct ion flux. For example, NMDARs can cooperate with mGluRs in the hippocampus to phosphorylate extracellular signal-regulated protein kinase (ERK) even when all ionotropic functions of the channel are prevented (Yang et al., 2004). Pore blockade by MK-801, chelation of intracellular Ca^{++} with BAPTA-AM, and exclusion of Ca^{++} and Na^{+} from the extracellular solution all failed to prevent the phosphorylation of ERK by co-activation of NMDARs (NMDA) and mGluRs (DHPG). In contrast, Yang et al. (2004) found that competitive block of the glutamate/NMDA binding site of NMDARs with AP5 successfully prevented ERK phosphorylation. Thus, the conformational changes following agonist binding to the glutamate/NMDA site must enable some metabotropic function in addition to channel opening.

Metabotropic function of NMDARs in activity-dependent plasticity has also been identified in acute hippocampal slices. Nabavi et al. (2013) found that LTD at synapses onto CA1 neurons induced by low-frequency stimulation (900 pulses, 1Hz) was NMDAR-dependent, independent of ion flux through the channels. This was verified by eliminating NMDAR ionotropic function in two ways: with MK-801, which blocks open NMDAR channels; and with the glycine binding-site competitive antagonist 7KC, which prevents channel opening. These two methods demonstrated that not only was ion flux through NMDAR channels unnecessary, but that glycine binding and the conformational changes required for channel opening were also not required. Thus, glutamate binding alone likely causes some separate conformational change that enables metabotropic activity.

If NMDARs are acting metabotropically at the AOB-MeA synapse, the 5Hz stimulation used in the present study should be adequate to activate them according to the results of Nabavi et al. (2013). This could explain their apparent effect on release probability at the resting synapse, without requiring conditions that allow channel opening. Therefore, I propose that NMDARs likely affect PPR at the AOB-MeA synapse through some metabotropic function.

4.1.4.2 Kainate receptors

An increase in PPR also accompanied the decrease in synaptic strength at the AOB-MeA synapse caused by bath application of the KAR antagonist UBP310. While GluK2/5 heteromers are predominantly post-synaptic, receptors containing the GluK1 subunit — which UBP310 was initially designed to block — are known to be located pre-synaptically (Paternain et al., 2000; Lauri et al., 2006; Shin et al., 2010; Clarke et al., 2014). Though GluK1-containing KARs are preferentially expressed in GABAergic interneurons in the hippocampus (Cossart et al., 1998; Wondolowski and Frerking, 2009) they have been shown to be located in glutamatergic synapses in the amygdala (Li et al.,

2001; Shin et al., 2010). In the amygdala these receptors have been implicated in the induction of pre-synaptically expressed LTP in response to repetitive low-frequency stimulation rather than negatively regulating release as they do in the hippocampus (Negrete-Díaz et al., 2006). It is possible that they may also act as auto-receptors at the AOB-MeA synapse, tonically facilitating release in response to ambient glutamate, which might explain why application of UBP310 seems to decrease probability of release.

If GluK1-containing KARs do indeed increase glutamate release at this synapse, they could do so by increasing $[Ca^{++}]_i$ in the terminal, either metabotropically through a G-protein cascade, or by supplementing evoked transient Ca^{++} influx ionotropically. Previous study of the AOB-MeA synapse found that neither blockade of NMDARs by AP5 nor AMPARs/KARs by CNQX, altered pre-synaptic Ca^{++} transients as measured by $\Delta F/F$ (change in fluorescence over resting fluorescence) of non-ratiometric Ca^{++} indicator dyes in response to single pulses or trains of stimuli (Mulligan, Davison and Delaney, 2001). However, fluorescence change measurements are less sensitive to differences in ambient $[Ca^{++}]_i$ than ratiometric measurements that make use of a second stable dye for comparison to the Ca^{++} reporting dye (Johnston and Delaney, 2010; Fekete et al., 2014). Therefore, KARs and NMDARs could still exercise their influence on release probability by slightly increasing basal/ambient $[Ca^{++}]_i$, which $\Delta F/F$ measurement of evoked transients might not have detected. In addition to being Ca^{++} permeable, GluK1-containing receptors can be linked with G-proteins coupled to PLC. Activation of PLC provides another route to increase $[Ca^{++}]_i$ in the pre-synaptic terminal or other modulations that could affect release probability, including cascades leading to the activation of protein kinases as well as direct activation of PKC by DAG (Rozas et al., 2003).

4.1.4.3 Possible means of induction and expression of LTP in the pre-synapse

The pre-synaptic LTP at the AOB-MeA hypothesized to underlie the long lasting (> 1 hour) decrease in PPR induced by 5Hz tetani is not blocked by bath application of

AP5 or UBP310, despite their apparent effects on release probability. As I propose for the post-synaptic component of LTP at this synapse, it may be that the conditions for induction can be met by multiple receptors/channels, such that blockade of one at a time is not sufficient to prevent LTP induction. This is the case at mossy fibre synapses in the hippocampus that express pre-synaptic LTP dependent on GluK1-containing and L-type voltage gated calcium channels (VGCCs) (Lauri et al., 2003). Researchers found induction of LTP by 50Hz stimulation to the dentate granule cell layer was insensitive to blockade of GluK1-containing KARs by the specific antagonist LY382884 or the L-type VGCC blocker nifedipine. However, LTP was prevented when LY3822884 and nifedipine were co-applied. When both channels were active, they cooperated to enable ryanodine sensitive Ca^{++} driven Ca^{++} release from intracellular stores, which lead to pre-synaptic LTP by some unidentified downstream mechanism.

One mechanism for expression of pre-synaptic LTP, manifested as a persistent enhancement of release probability, is modification of the active zone protein RIM1α by PKA activated through cAMP signalling (Fourcaudot et al., 2008). Fourcaudot et al. found this pathway responsible for the expression of NMDAR-dependent LTP in cortical inputs to lateral amygdala neurons. Although not confirmed in their study, increased $[Ca^{++}]_i$ resulting from activation of NMDARs likely started the required cascade involving Ca^{++} sensitive adenylyl cyclase generating cAMP to activate PKA. PKA is known to target the active zone protein RIM1α, which is important for Ca^{++}-release coupling and the expression of some forms of pre-synaptic LTP (Schoch et al., 2002; Chevaleyre et al., 2007; Fourcaudot et al., 2008). Dependence of NMDAR-PKA-dependent pre-synaptic LTP on RIM1α was supported by a lack of pre-LTP in RIM1α$^{-/-}$ mice, while post-synaptic LTP remained intact.

I suspect that the LTP related increase in release probability observed at the AOB-MeA synapse could be dependent on the activation of PKA due to its involvement in other instances of pre-synaptic LTP and also the presence of two potential activators in the pre-synaptic terminal at this synapse. Firstly, KARs can be both Ca^{++} permeable and linked with G-proteins that lead to additional increases in $[Ca^{++}]_i$ (Rozas et al., 2003).

Secondly, NMDARs provide another means by which the required Ca^{++} influx can occur. While blockade of either of these receptors separately did not prevent lasting decreases in PPR or impair LTP induction, one may be able to cover for the other as demonstrated with GluK1-containing KARs and L-type VGCCs by Lauri et al. (2003).

4.2 Future Directions

The present study established that there is a form of LTP inducible by 5Hz tetani (and by 1Hz, though the mechanisms may be different) at the AOB-MeA synapse of *L. catesbeiana.* The data collected are consistent with both pre-synaptic and post-synaptic loci of expression. Based on changes in PPR and the effects of the KAR blocker UBP310, I have proposed a model in which pre-synaptic probability of release is increased and the post-synaptic KAR response is enhanced. Additional research must be conducted to test these assumptions, confirm the mode of participation of both sides of the synapse and determine the key mechanisms for induction and expression of this AOB-MeA LTP.

4.2.1 Tonic facilitation of pre-synaptic release by KARs and NMDARs

Both UBP310 and AP5 were found to increase PPR (Figure 5E; Figure 6), which is consistent with a decrease in probability of release. This implies that both KARs and NMDARs are tonically increasing neurotransmitter release at the AOB-MeA synapse. While a decrease in PPR has been linked to an increase in probability of release at synapses with moderate to high initial release probability (Delaney et al., 1989; Zucker and Regehr, 2002), PPR of tract evoked field recordings is not the most direct measurement of release. Increases in probability of release will not necessarily be reported by a change in PPR if the amount of release is not high enough to tax the readily releasable pool of vesicles (Hanse and Gustafsson, 2001). Also, use of evoked activity to measure release probability is not ideal because the surrounding network of neurons

outside of the terminal of interest, such as GABA-releasing interneurons, could also be activated either directly or di-synaptically to affect release initiated by repeated stimuli (Murphy et al., 2004; Delaney et al., 2009). Thus, additional measurements to supplement the paired-pulse field recordings of the present study will be necessary to further characterize the pre-synaptic action of KARs and NMDARs at this synapse.

The coefficient of variation (CV) is one such measurement that can be employed alongside PPR that can inform on changes to pre-synaptic release probability. CV is calculated from the fluctuation of whole-cell EPSCs generated by minimal stimulation of pre-synaptic neurons/fibres (Malinow and Tsien, 1990). Since stimulation is weak, the number of pre-synaptic terminals brought towards their thresholds will be fewer, thus the post-synaptic response will be very dependent on the probability of neurotransmitter release from the pre-synaptic terminals stimulated. Large CVs are indicative of low probabilities of release, because release failing more frequently creates a wider range of post-synaptic outcomes. Conversely, lower CVs are indicative of high release probability because the amount of release between stimuli repetitions is more reliable. Measuring CV at the AOB-MeA synapse before and during UBP310 and AP5 application could provide secondary confirmation of the suspected pre-synaptic effects of KARs and NMDAR. Increases in CV following antagonism of these receptors would be consistent with decreased probability of release (Choi and Lovinger, 1997) as implied by the increase in PPR previously observed. These experiments will require whole-cell recordings of MeA neurons in voltage clamp configuration. Mulligan et al. (2001) recorded from blindly patched MeA neurons in *L. pipiens*, and found 45% of the successfully patched neurons received mono-synaptic inputs from AOB mitral cells. Thus, the proposed measurements of CV are plausible, although more taxing due to the length of recordings required for LTP experiments.

Whole-cell recordings of MeA neurons should also be performed to observe whether spontaneous asynchronous release events from AOB mitral cell terminals are sensitive to antagonism of KARs or NMDARs. Isolation of the asynchronous release and the mEPSCs it evokes is achieved through the use of the voltage-gated Na+ channel

blocker tetrodotoxin (TTX). By blocking Na^+ channels, TTX prevents the generation and propagation of APs, isolating the pre-synaptic terminal from AP-reliant network activity that could drive release. Thus, any post-synaptic currents (mEPSCs) recorded in the presence of TTX are generated by spontaneously occurring asynchronous release of neurotransmitters. Changes in the frequency of mEPSCs are commonly interpreted as due to changes in the intrinsic probability of release of the pre-synaptic terminal (Malgaroli and Tsien, 1992; Bolshakov and Siegelbaum, 1995). Conversely, changes in the amplitude of mEPSCs are often considered representative of changes in the post-synaptic response to neurotransmitter release (O'Brien et al., 1998). Frequency and amplitude of mEPSCs in the presence of TTX should be recorded before and after separate application of UBP310 and AP5 to observe the activity of KARs and NMDARs during rest. If application of an antagonist decreases the frequency of mEPSCs it would be consistent with the corresponding receptor contributing to tonic release facilitation. Confirmatory applications of the KAR agonist ATPA and the NMDAR agonist NMDA should then have the opposite effect, increasing mEPSC frequency. However, a result in which mEPSC frequency is not decreased by antagonism of either KAR or NMDAR antagonism would suggest that the effect of the receptor on PPR is not directly on the terminal and is dependent on TTX-sensitive network activity.

4.2.1.1 Mode of action of NMDARs: Ionotropic or metabotropic

In the event that AP5 application decreases mEPSC frequency, bath application of the non-competitive use-dependent NMDAR pore-blocker MK-801 could help to further characterize the behaviour of NMDARs at the AOB-MeA synapse. MK-801 will only enter and block NMDAR channels if they are currently open for ion flux, leaving any closed and inactive channels unaffected. Thus, if MK-801 increases CV or decreases mEPSC frequency it would be consistent with pre-synaptic NMDARs being open at rest in the absence of spontaneous or evoked APs. Pore blockade having an effect on CV or mEPSC frequency would also demonstrate that NMDARs are likely affecting release through fluxing Ca^{++} ions into the terminal. If MK-801 does not increase CV or decrease mEPSC frequency (but AP5 does) it would suggest that the effect of NMDARs on the

pre-synaptic terminal may be Ca^{++} flux independent. A metabotropic function of pore-blocked NMDARs has been previously reported, indicating that ligand binding on its own may be sufficient to activate some of the receptors functions (Yang et al., 2004; Kessels et al., 2013; Nabavi et al., 2013; Birnbaum et al., 2015). If NMDARs are acting metabotropically to increase probability of release at the AOB-MeA synapse, the agonist NMDA should decrease CV and increase mEPSC frequency from terminals already pore-blocked by MK-801.

4.2.3 Post-synaptic KAR mediated LTP expression

Of the data collected in the present study, the enhanced effect of the KAR blocker UBP310 following induction of LTP by 5Hz tetani provides the most information regarding the post-synaptic mechanisms of LTP expression at the AOB-MeA synapse. However the comparison of fEPSPs with and without UBP310 before and after 5Hz tetani only provides an indirect measure of the change in KAR mediated post-synaptic current. A more accurate representation of KAR mediated post-synaptic current should be obtained through pharmacological isolation of the KAR current from other glutamate receptor currents. Isolated KAR mEPSCs would then be recorded whole-cell in tetanus-naive and tetanus-potentiated MeA neurons to observe whether more current is being fluxed by KARs during expression of LTP.

Both AMPARs and NMDARs would need to be blocked for a complete isolation of KAR currents, however only blocking AMPARs may be a more feasible solution. The specific NMDAR antagonist AP5 is suspected to decrease probability of release at the AOB-MeA synapse (Figure 5E), so KAR currents would also be reduced. Fortunately, antagonism of AMPAR receptors, thereby reducing post-synaptic depolarization, may be sufficient to limit ion flux through NMDARs at the AOB-MeA synapse (Mulligan et al., 2001). The non-competitive AMPAR antagonist GYKI-52466, highly selective for AMPARs (IC_{50} ~10-20μM) over KARs (IC_{50} ~450μM) (Paternain et al., 1995), should be sufficient to partially isolate KAR currents. Thus, the ratio of AMPAR inclusive to

AMPAR exclusive post-synaptic responses could roughly report the proportion of the post-synaptic response due to KARs.

KAR fEPSPs, partially isolated with GYKI-52466, should be recorded before and 30 minutes after delivery of 5Hz tetani to the AOT. The antagonist would be applied to the tetanus-naive synapse to record AMPAR-independent fEPSPs and then washed out before delivery of 5Hz stimulation, so as not to interfere with induction. After 30 minutes post 5Hz stimulation, GYKI-52466 would be bath-applied to partially isolate the post-synaptic KAR response once more. Increased size of predominantly KAR fEPSPs in the presence of the AMPAR antagonist relative to control fEPSPs post-tetanus would support a role for increased KAR mediated currents in LTP.

Should the pre-synaptic effect of NMDARs at the AOB-MeA synapse turn out to be metabotropic (see 4.2.1.1), the above experiment could be refined with the added block of NMDARs. The pore-blocker MK-801 could be co-applied with GYKI-52466 for a more complete isolation of post-synaptic KAR currents without also decreasing pre-synaptic release. Whole-cell recording of pharmacologically isolated KAR EPSCs would be an excellent follow-up experiment should this simpler method support a 5Hz induced increase in KAR current. However, maintaining a blind whole-cell patch for the duration required for these LTP experiments with multiple drug applications would be taxing and is best left for secondary confirmation experiments.

4.2.4 Prevention of LTP induction

If KARs are contributing more to the MeA fEPSP following 5Hz tetani, the post-synaptic mechanisms responsible for generating the change at the AOB-MeA synapse may be similar to those found in rat neuron cultures where KAR functions and populations have been altered by stimulation of group 1 mGluRs (Rojas et al., 2013) and

KARs (González-González and Henley, 2013). In both cortical and hippocampal neuron cultures, regardless of the glutamate receptor involved, inhibition of G-proteins, chelation of Ca^{++} and inhibition of PKC all prevented the chemically induced KAR trafficking and/or potentiation. Given this information, I hypothesize that induction of post-synaptic LTP by sets of 5Hz tetani at the AOB-MeA could be prevented by interfering with the above mechanisms.

4.2.4.1 Simultaneous blockade of KARs, NMDARs, group 1 mGluRs, and L-type VGCCs

The downstream target proteins responsible for initiating expression of LTP at the AOB-MeA synapse are unknown. Protein kinases that have been previously identified as agents in pre- and/or post-synaptic LTP, such as PKC (Malinow et al., 1989; Luu and Malenka, 2008), PKA (Fourcaudot et al., 2008) and CaMKII (Malinow et al., 1989), can share upstream factors that signal for their activation. The increases of $[Ca^{++}]_i$ and the activation of membrane-bound proteins required for the cascade of these kinases can be achieved by multiple receptors and channels in the membrane. Therefore, our next experiments should pharmacologically target a selection of membrane proteins that might serve as the first steps in LTP induction.

In the present study, AP5 and UBP310 were applied separately to observe their effects on the AOB-MeA synapse and the role NMDARs and KARs in 5Hz induced LTP. Neither antagonist on its own was sufficient to block LTP induction, but if both glutamate receptors are exerting their intracellular effects through shared second messengers, one might compensate for the blockade of the other. In fact, LTP induction redundancies have been observed previously at the mossy fibre-CA3 synapse in the hippocampus. In separate studies it has been found that combined blockade of KARs and L-type VGCCs (Lauri et al., 2003) and combined blockade of KARs and mGluRs (Wallis et al., 2015) prevent LTP induction, whereas separately antagonising the same receptors/channels does not. Thus, despite the present result that UBP310 and AP5 do not

prevent LTP induction at the AOB-MeA, both antagonists should be applied alongside others that are yet to be tested in order to confirm this observation.

I propose that KARs (UBP310), NMDARs (AP5), group 1 mGluRs (MCPG), and L-type VGCCs (nifedipine) should be blocked simultaneously before 5Hz tetanic stimulation using the same paradigm as the experiments presented in Figure 7. All of these targets have been linked to instances of both pre- and post-synaptic induction of LTP, thus their combined application will serve as a wide net to catch the key components responsible for 5Hz induced AOB-MeA LTP. As was done in my previous experiments, initial pre-drug and pre-tetanus fEPSP slopes would be compared to slopes > 1 hour after 5Hz stimulation once the drugs have been washed out. A significant reduction in LTP strength by the combination of UBP310, AP5, MCPG, and nifedipine compared to control experiments without the antagonists would be consistent with group 1 mGluRs, L-type VGCCs, or some combination of the four membrane proteins being required for induction.

If LTP is only partially blocked, further assessment by PPR, CV and mEPSC frequencies could be performed to establish whether the remaining LTP is being expressed pre- or post-synaptically. For field recording experiments, a decrease in PPR following 5Hz tetani would be consistent with a preserved pre-synaptic LTP, but further characterization with whole-cell recordings would strengthen this conclusion. Whole-cell voltage-clamp recordings of EPSCs generated by minimal stimulation to calculate CV could be used as secondary confirmation of changes in probability of release should PPR be decreased. Lastly and most technically difficult, frequency and amplitude of mEPSCs could be measured in whole-cell experiments with TTX before and after 5Hz tetani delivered in the presence of UBP310, AP5, MCPG and nifedipine. An increase in mEPSC frequency and no increase in amplitude would be consistent with preserved induction of pre-synaptic LTP and blocked post-synaptic LTP (O'Brien et al., 1998), while the reverse would indicate only post-synaptic LTP remained.

Pending partial or complete prevention of LTP induction by the combination of antagonists, further experiments could probe for the key receptor/channel or combination thereof required by using different permutations of the antagonists. If post-synaptic LTP is not blocked, experiments directed at a key secondary messenger such as Ca^{++} may be appropriate to confirm induction is indeed post-synaptic and narrow down the subsequent search for the membrane protein(s) necessary for induction of LTP.

4.2.4.2 Post-synaptic Ca^{++} chelation

Increases in post-synaptic $[Ca^{++}]_i$ could be prevented to determine if the ion is required as a messenger for the induction of post-synaptic LTP, as it is at CA3-CA1 hippocampal neurons (Lynch et al., 1983). This can be done by inclusion of the membrane impermeable Ca^{++} chelator BAPTA in the intracellular solution during whole-cell recordings. By quickly buffering $[Ca^{++}]_i$ transients, BAPTA can limit or prevent the activation of LTP-associated, Ca^{++}-dependent proteins such as adenylyl cyclase and PKC (Luu and Malenka, 2008; González-González and Henley, 2013). If induction of post-synaptic LTP is dependent on Ca^{++} at this synapse, the presence of intracellular BAPTA should prevent it and leave pre-synaptic LTP intact. Based on the proportion of LTP expressed in the presence of UBP310 (Figure 7), I estimate the magnitude of pre-synaptic LTP at this synapse to be 1.4 fold out of a total 1.7 fold (Figure 10). Therefore, I hypothesize 5Hz tetani would induce a similar magnitude (~1.4-fold) of LTP in the presence of BAPTA if it successfully blocks post-synaptic LTP. In this scenario, LTP expressed after 5Hz tetanus with post-synaptic BAPTA should be associated with a decrease in PPR, a decrease in CV, and an increase in the frequency but not the amplitude of mEPSCs.

Bibliography

Adolphs R, Tranel D, Damasio H, Damasio AR (1995) Fear and the human amygdala. J Neurosci 15:5879–5891.

Andrásfalvy BK, Magee JC (2004) Changes in AMPA receptor currents following LTP induction on rat CA1 pyramidal neurones. J Physiol 559:543–554.

Bach EC, Smith BN (2012) Presynaptic NMDA receptor-mediated modulation of excitatory neurotransmission in the mouse dorsal motor nucleus of the vagus. J Neurophysiol 108:1484–1491

Berner NJ (1999) Oxygen consumption by mitochondria from an endotherm and an ectotherm. Comp Biochem Physiol - B Biochem Mol Biol 124:25–31.

Berretta N, Jones RSG (1996) Tonic facilitation of glutamate release by presynaptic N-methyl-D-aspartate autoreceptors in the entorhinal cortex. 75:339–344.

Berridge MJ (1993) Inositol trisphosphate and calcium signalling. Nature 361:315–325.

Birnbaum JH, Bali J, Rajendran L, Nitsch RM, Tackenberg C (2015) Calcium flux-independent NMDA receptor activity is required for Aβ oligomer-induced synaptic loss. Cell Death Dis 6:e1791

Bliss T V, Collingridge GL (1993) A synaptic model of memory: Long-term potentiation in the hippocampus. Nature 361:31–39.

Bolshakov VY, Siegelbaum SA (1995) Regulation of hippocampal transmitter release during development and long-term potentiation. Science (80-) 269:1730–1734.

Brager DH, Cai X, Thompson SM (2003) Activity-dependent activation of presynaptic protein kinase C mediates post-tetanic potentiation. Nat Neurosci 6:551–552

Byth LA (2014) Ca2+- and CaMKII-mediated processes in early LTP. Ann Neurosci 21:151–153 Available at:

Chevaleyre V, Heifets BD, Kaeser PS, Südhof TC, Purpura DP, Castillo PE (2007) Endocannabinoid-mediated long-term plasticity requires cAMP/PKA signaling and RIM1α. Neuron 54:801–812

Cho J-H, Bayazitov IT, Meloni EG, Myers KM, Carlezon WA, Zakharenko SS, Bolshakov VY (2011) Coactivation of thalamic and cortical pathways induces input timing–dependent plasticity in amygdala. Nat Neurosci 15:113–122

Choi DW (1987) Ionic dependence of glutamate neurotoxicity. J Neurosci 7:369–379.

Choi S, Lovinger DM (1997) Decreased probability of neurotransmitter release underlies striatal long-term depression and postnatal development of corticostriatal synapses. Proc Natl Acad Sci U S A 94:2665–2670.

Clarke VRJ, Molchanova SM, Hirvonen T, Taira T, Lauri SE (2014) Activity-dependent upregulation of presynaptic kainate receptors at immature CA3-CA1 synapses. J Neurosci 34:16902–16916

Cossart R, Esclapez M, Hirsch JC, Bernard C, Ben-Ari Y (1998) GluR5 kainate receptor activation in interneurons increases tonic inhibition of pyramidal cells. Nat Neurosci 1:470–478.

Debanne D, Guérineau NC, Gähwiler BH, Thompson SM (1996) Paired-pulse facilitation and depression at unitary synapses in rat hippocampus: quantal fluctuation affects subsequent release. J Physiol 491.1:163–176.

Delaney K, Davison I, Denk W (2001) Odour-evoked [Ca2+] transients in mitral cell dendrites of frog olfactory glomeruli. Eur J Neurosci 13:1658–1672.

Delaney KR, Hall BJ (1996) An in vitro preparation of frog nose and brain for the study of odour-evoked oscillatory activity. J Neurosci Methods 68:193–202.

Delaney KR, Qnais EY, Hardy AB (2009) Short-term synaptic plasticity at the main and vomeronasal olfactory receptor to mitral cell synapse in frog. Eur J Neurosci 30:2077–2088

Delaney KR, Zucker RS, Tank DW (1989) Calcium in motor nerve terminals associated with posttetanic potentiation. J Neurosci 9:3558–3567.

Dobrunz LE, Huang EP, Stevens CF (1997) Very short-term plasticity in hippocampal synapses. Proc Natl Acad Sci U S A 94:14843–14847.

Dobrunz LE, Stevens CF (1997) Heterogeneity of release probability, facilitation, and depletion at central synapses. Neuron 18:995–1008.

Dudek SM, Bear MF (1992) Homosynaptic long-term depression in area CA1 of hippocampus and effects of N-methyl-D-aspartate receptor blockade. Proc Natl Acad Sci U S A 89:4363–4367.

Espinosa F, Kavalali ET (2009) NMDA receptor activation by spontaneous glutamatergic neurotransmission. J Neurophysiol 101:2290–2296.

Faden AI, Demediuk P, Panter SS, Vink R (1989) The role of excitatory amino acids and NMDA receptors in traumatic brain injury. Science (80-) 244:798–800.

Fekete A, Johnston J, Delaney KR (2014) Presynaptic T-Type Ca2+ channels modulate dendrodendritic mitral-mitral and mitral-periglomerular connections in mouse olfactory bulb. J Neurosci 34:14032–14045

Feldman DE (2012) The spike-timing dependence of plasticity. Neuron 75:556–571

Fioravante D, Chu Y, de Jong AP, Leitges M, Kaeser PS, Regehr WG (2014) Protein kinase C is a calcium sensor for presynaptic short-term plasticity. Elife 3:e03011

Fioravante D, Regehr WG (2011) Short-term forms of presynaptic plasticity. Curr Opin Neurobiol 21:269–274.

Fourcaudot E, Gambino F, Humeau Y, Casassus G, Shaban H, Poulain B, Luthi A (2008) cAMP / PKA signaling and RIM1α mediate presynaptic LTP in the lateral amygdala. PNAS 105:15130–15135.

Fritsch B, Reis J, Gasior M, Kaminski RM, Rogawski MA (2014) Role of GluK1 kainate receptors in seizures, epileptic discharges, and epileptogenesis. J Neurosci 34:5765–5775

Genç Ö, Kochubey O, Toonen RF, Verhage M, Schneggenburger R (2014) Munc18-1 is a dynamically regulated PKC target during short-term enhancement of transmitter release. Elife 2014:1–19.

Goddard G V, McIntyre DC, Leech CK (1969) A permanent change in brain function resulting from daily electrical stimulation. Exp Neurol 25:295–330.

González-González IM, Henley JM (2013) Postsynaptic kainate receptor recycling and surface expression are regulated by metabotropic autoreceptor signalling. Traffic 14:810–822.

Habib D, Dringenberg HC (2009) Alternating low frequency stimulation of medial septal and commissural fibers induces NMDA-dependent, long-lasting potentiation of hippocampal synapses in urethane-anesthetized rats. Hippocampus 19:299–307

Habib D, Dringenberg HC (2010a) Low-frequency-induced synaptic potentiation: a paradigm shift in the field of memory-related plasticity mechanisms? Hippocampus 20:29–35

Habib D, Dringenberg HC (2010b) Surprising similarity between mechanisms mediating low (1 Hz)-and high (100 Hz)-induced long-lasting synaptic potentiation in CA1 of the intact hippocampus. Neuroscience 170:489–496

Hanse E, Gustafsson B (2001) Paired-pulse plasticity at the single release site level: an experimental and computational study. J Neurosci 21:8362–8369.

Huang Y-Y, Kandel ER (2007) Low-frequency stimulation induces a pathway-specific late phase of LTP in the amygdala that is mediated by PKA and dependent on protein synthesis. Learn Mem 14:497–503

Huettner JE (2003) Kainate receptors and synaptic transmission. Prog Neurobiol 70:387–407 Available at: http://linkinghub.elsevier.com/retrieve/pii/S0301008203001229 [Accessed April 2, 2014].

Johnston J, Delaney KR (2010) Synaptic activation of T-type Ca2+ channels via mGluR activation in the primary dendrite of mitral cells. J Neurophysiol 103:2557–2569.

Katayama Y, Becker DP, Tamura T, Hovda DA (1990) Massive increases in extracellular potassium and the indiscriminate release of glutamate following concussive brain injury. J Neurosurg 73:889–900.

Kelso SR, Ganong AH, Brown TH (1986) Hebbian synapses in hippocampus. Proc Natl Acad Sci U S A 83:5326–5330.

Kessels HW, Nabavi S, Malinow R (2013) Metabotropic NMDA receptor function is required for beta-amyloid-induced synaptic depression. Proc Natl Acad Sci U S A 110:4033–4038

Laberge F, Mühlenbrock-lenter S, Grunwald W, Roth G (2006) Evolution of the amygdala : New insights from studies in amphibians. Brain, Behav Evol 67:177–187.

Lanté F, Ferreira M-C, Guiramand J, Recasens M, Vignes M (2006) Low-frequency stimulation induces a new form of LTP , metabotropic glutamate (mGlu 5) receptor- and PKA-dependent , in the CA1 area of the rat hippocampus. Hippocampus 360:345–360.

Larson J, Munkácsy E (2014) Theta-burst LTP. Brain Res:1–13

Lauri SE, Bortolotto ZA, Nistico R, Bleakman D, Ornstein PL, Lodge D, Isaac JTR, Collingridge GL (2003) A role for Ca 2+ stores in kainate receptor-dependent synaptic facilitation and LTP at mossy fiber synapses in the hippocampus. Neuron 39:327–341.

Lauri SE, Vesikansa A, Segerstråle M, Collingridge GL, Isaac JTR, Taira T (2006) Functional maturation of CA1 synapses involves activity-dependent loss of tonic kainate receptor-mediated inhibition of glutamate release. Neuron 50:415–429.

LeDoux JE, Iwata J, Cicchetti P, Reis DJ (1988) Different projections of the central amygdaloid nucleus mediate autonomic and behavioral correlates of conditioned fear. J Neurosci 8:2517–2529.

Lerma J (2006) Kainate receptor physiology. Curr Opin Pharmacol 6:89–97.

Li H, Chen A, Xing G, Wei M, Rogawski MA (2001) Kainate receptor-mediated heterosynaptic facilitation in the amygdala. Nat Neurosci 4:612–620.

Luksch H, Walkowiak W, Munoz A, Donkelaar HJ, Wallen Ž (1996) The use of in vitro preparations of the isolated amphibian central nervous system in neuroanatomy and electrophysiology.

Luu P, Malenka RC (2008) Spike timing-dependent long-term potentiation in ventral tegmental area dopamine cells requires PKC. J Neurophysiol 100:533–538.

Lynch G, Larson J, Kelso SR, Barrionuevo G, Schottler F (1983) Intracellular injections of EGTA block induction of hippocampal long-term potentiation. Nature 305:719–721.

Malenka RC (1991) Postsynaptic factors control the duration of synaptic enhancement in area CA1 of the hippocampus. Neuron 6:53–60

Malgaroli A, Tsien R (1992) Glutamate-induced long-term potentiation of the frequency of miniature synaptic currents in cultured hippocampal neurons. Nature:134–139

Malinow R, Madison D V, Tsien RW (1988) Persistent protein kinase activity underlying long-term potentiation. Nature 335:820–824.

Malinow R, Schulman H, Tsien RW (1989) Inhibition of postsynaptic PKC or CaMKII blocks induction but not expression of LTP. Science (80-) 245:862–866.

Malinow R, Tsien RW (1990) Presynaptic enhancement shown by whole-cell recordings of long-term potentiation in hippocampal slices. Nature 346:177–180.

Mayford M, Wang J, Kandel ER, O'Dell TJ (1995) CaMKII regulates the frequency-response function of hippocampal synapses for the production of both LTD and LTP. Cell 81:891–904.

McGuinness L, Taylor C, Taylor RDT, Yau C, Langenhan T, Hart ML, Christian H, Tynan PW, Donnelly P, Emptage NJ (2010) Presynaptic NMDARs in the hippocampus facilitate transmitter release at theta frequency. Neuron 68:1109–1127

Moreno N, González A (2003) Hodological characterization of the medial amygdala in a nuran amphibians. J Comp Neurol 466:389–408.

Moreno N, González A (2004) Localization and connectivity of the lateral amygdala in anuran amphibians. J Comp Neurol 479:130–148.

Mulligan SJ, Davison I, Delaney KR (2001) Mitral cell presynaptic Ca(2+) influx and synaptic transmission in frog amygdala. Neuroscience 104:137–151

Murphy GJ, Glickfeld LL, Balsen Z, Isaacson JS (2004) Sensory neuron signaling to the brain: properties of transmitter release from olfactory nerve terminals. J Neurosci 24:3023–3030.

Nabavi S, Kessels HW, Alfonso S, Aow J, Fox R, Malinow R (2013) Metabotropic NMDA receptor function is required for NMDA receptor-dependent long-term depression. Proc Natl Acad Sci U S A 110:4033–4038

Negrete-Díaz J V, Sihra TS, Delgado-García JM, Rodríguez-Moreno A (2006) Kainate receptor-mediated inhibition of glutamate release involves protein kinase A in the mouse hippocampus. J Neurophysiol 96:1829–1837.

Nowak L, Bregestovski P, Ascher P, Herbet A, Prochiantz A (1984) Magnesium gates glutamate-activated channels in mouse central neurones. Nature 307:462–465.

O'Brien RJ, Kamboj S, Ehlers MD, Rosen KR, Fischbach GD, Huganir RL (1998) Activity-dependent modulation of synaptic AMPA receptor accumulation. Neuron 21:1067–1078.

O'Donovan MJ, Ho S, Sholomenko G, Yee W (1993) Real-time imaging of neurons retrogradely and anterogradely labelled with calcium-sensitive dyes. J Neurosci Methods 46:91–106.

Pape H, Pare D (2010) Plastic Synaptic Networks of the Amygdala for the Acquisition , Expression , and Extinction of Conditioned Fear. Physiol Rev 90:419–463.

Papes F, Logan DW, Stowers L (2010) The vomeronasal organ mediates interspecies defensive behaviors through detection of protein pheromone homologs. Cell 141:692–703.

Paternain A V, Herrera MT, Nieto MA, Lerma J (2000) GluR5 and GluR6 kainate receptor subunits coexist in hippocampal neurons and coassemble to form functional receptors. J Neurosci 20:196–205.

Paternain A V, Morales M, Lerma J (1995) Selective antagonism of AMPA receptors unmasks kainate receptor-mediated responses in hippocampal neurons. Neuron 14:185–189.

Pinheiro PS, Lanore F, Veran J, Artinian J, Blanchet C, Crépel V, Perrais D, Mulle C (2013) Selective block of postsynaptic kainate receptors reveals their function at hippocampal mossy fiber synapses. Cereb Cortex 23:323–331

Regehr WG, Delaney R, Tank DW (1994) The role of presynaptic calcium in short-term enhancement at the hippocampal mossy fiber synapse. J Neurosci 14:523–537.

Rodríguez-Durán LF, Escobar ML (2014) NMDA receptor activation and PKC but not PKA lead to the modification of the long-term potentiation in the insular cortex induced by conditioned taste aversion: Differential role of kinases in metaplasticity. Behav Brain Res 266:58–62

Rodríguez-Moreno A, Sihra TS (2007) Kainate receptors with a metabotropic modus operandi. Trends Neurosci 30:630–637.

Rodríguez-moreno A, Sihra TS (2011) Kainate receptors. In: Kainate Receptors: Novel Signaling Insights.

Rojas A, Wetherington J, Shaw R, Serrano G, Swanger S, Dingledine R (2013) Activation of group I metabotropic glutamate receptors potentiates heteromeric kainate receptors. Mol Pharmacol 83:106–121

Rosenzweig ES, Rao G, McNaughton BL, Barnes C a (1997) Role of temporal summation in age-related long-term potentiation- induction deficits. Hippocampus 7:549–558.

Rozas JL, Paternain A V., Lerma J (2003) Noncanonical signaling by ionotropic kainate receptors. Neuron 39:543–553.

Scalia F (1972) The projection of the accessory olfactory bulb in the frog. Brain Res 36:409–411.

Scalia F, Gallousis G, Roca S (1991) Differential projections of the main and accessory olfactory bulb in the frog. J Comp Neurol 305:443–461.

Schoch S, Castillo PE, Jo T, Mukherjee K, Geppert M, Wang Y, Schmitz F, Malenka RC, Südhof TC (2002) RIM1α forms a protein scaffold for regulating neurotransmitter release at the active zone. Nature 415:321–326.

Seidl a. H (2013) Regulation of conduction time along axons. Neuroscience 276:126–134

Shin R, Tully K, Li Y, Cho J, Higuchi M, Suhara T, Vadim Y, Bolshakov VY (2010) Hierarchical order of coexisting pre- and postsynaptic forms of long-term potentiation at synapses in amygdala. Proc Natl Acad Sci U S A 107:19073–19078

Steven R (1984) Synaptic release of excitatory amino acid neurotransmitter mediates axonic neuronal death. J Neurosci 4:1884–1891.

Wallis JL, Irvine MW, Jane DE, Lodge D, Collingridge GL, Bortolotto ZA (2015) An interchangeable role for kainate and metabotropic glutamate receptors in the

induction of rat hippocampal mossy fiber long-term potentiation in vivo. Hippocampus 00:1–11

Wondolowski J, Frerking M (2009) Subunit-dependent postsynaptic expression of kainate receptors on hippocampal interneurons in area CA1. J Neurosci 29:563–574.

Yang L, Mao L, Tang Q, Samdani S, Liu Z, Wang JQ (2004) A novel Ca2+-independent signaling pathway to extracellular signal-regulated protein kinase by coactivation of NMDA receptors and metabotropic glutamate receptor 5 in neurons. J Neurosci 24:10846–10857.

Zucker RS, Regehr WG (2002) Short-term synaptic plasticity. Annu Rev Physiol 64:355–405.